Unparalleled Contribtions of 18F-FDG-PET Imaging to Medicine Over the Past Four Decades

Abass Alavi,M.D.

M.D.(Hon),Ph.D.(Hon),D.Sc.(Hon)

Perelman School of Medicine, University of Pennsylvania, Philadelphia, Pennsylvania

How did this journey begin and where is it heading?

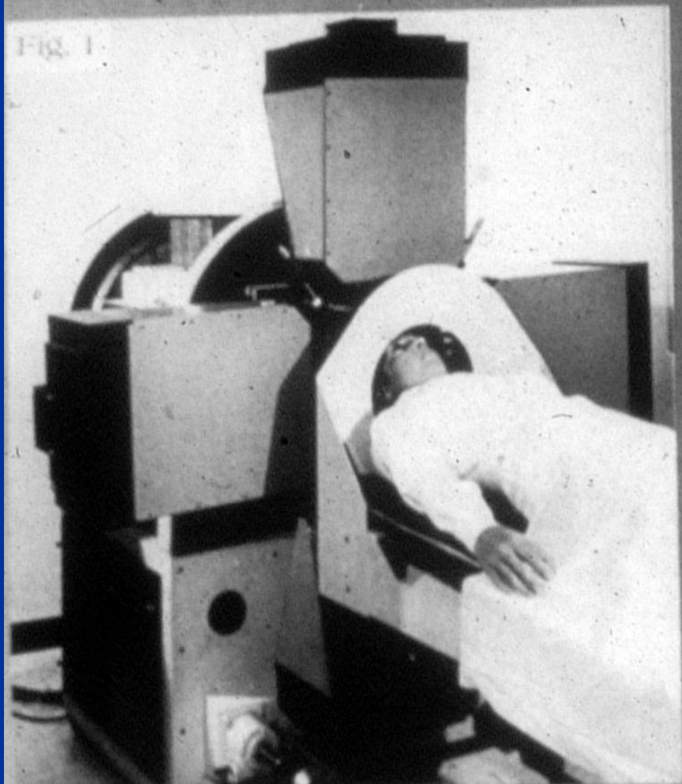
Fig. 1

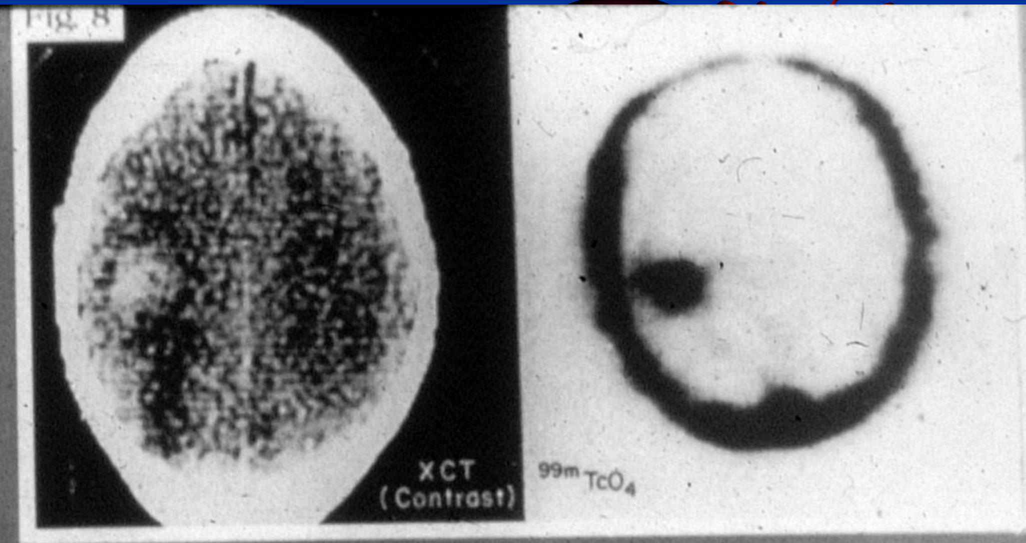
Fig. 8
XCT
(Contrast)
$^{99m}TcO_4$

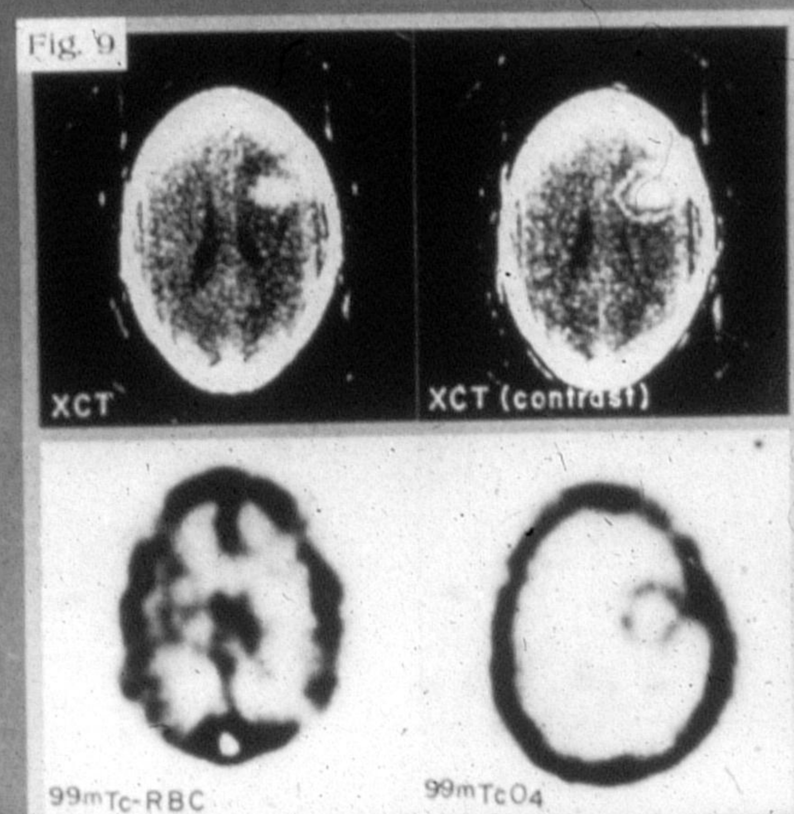
Fig. 9
XCT
XCT (contrast)
^{99m}Tc-RBC
$^{99m}TcO_4$

14C-deoxyglucose autoradiography

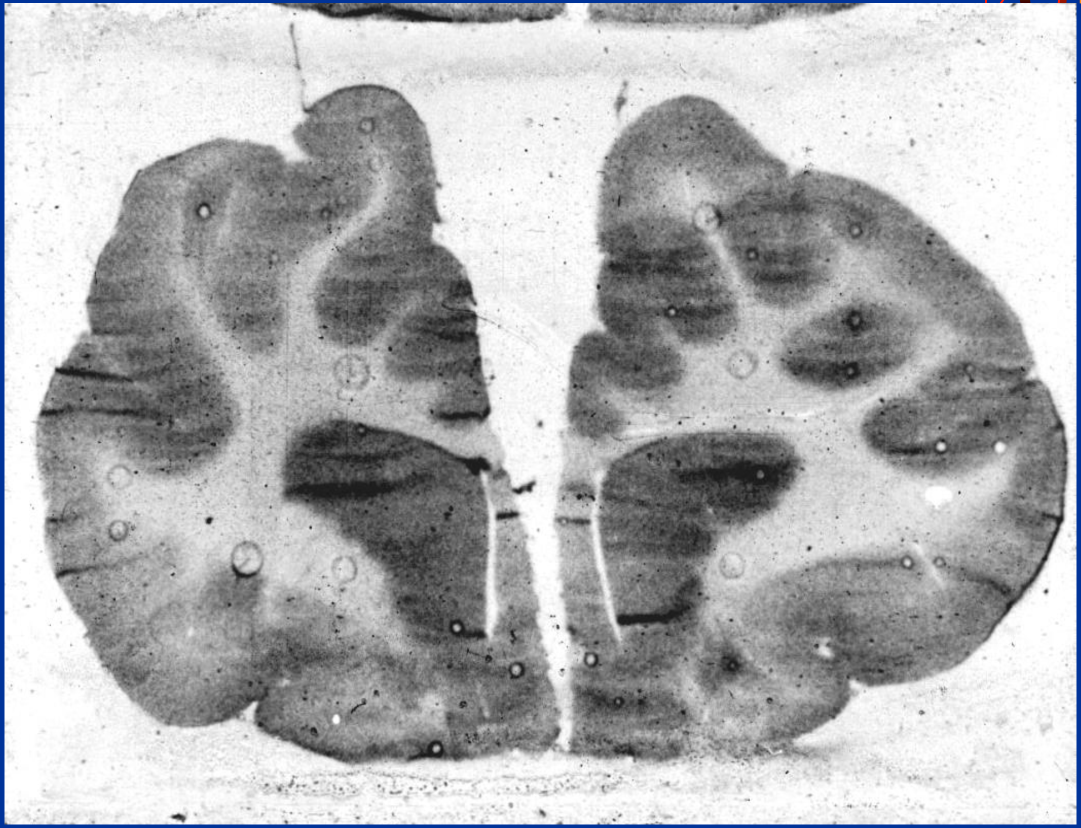

14C-deoxyglucose autoradiography

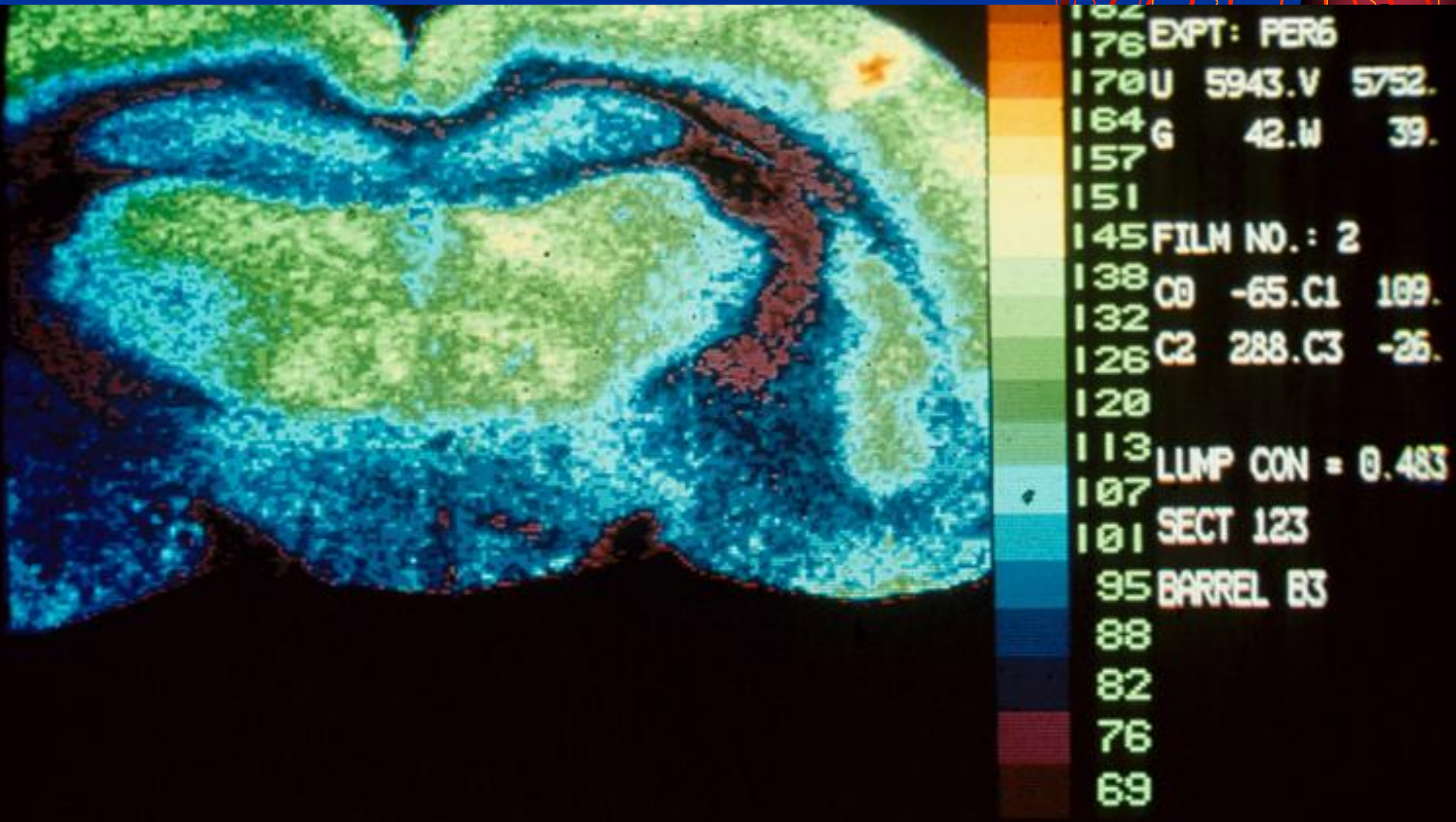

Concept of Fluorodeoxyglucose (FDG)

Alavi, Kuhl, Reivich
(University of Pennsylvania)

Wolf, Ido, Fowler
(Brookhaven National Laboratory)

December 1973

[^{18}F] FDG – the Molecule of the Century
Uptake and Metabolism

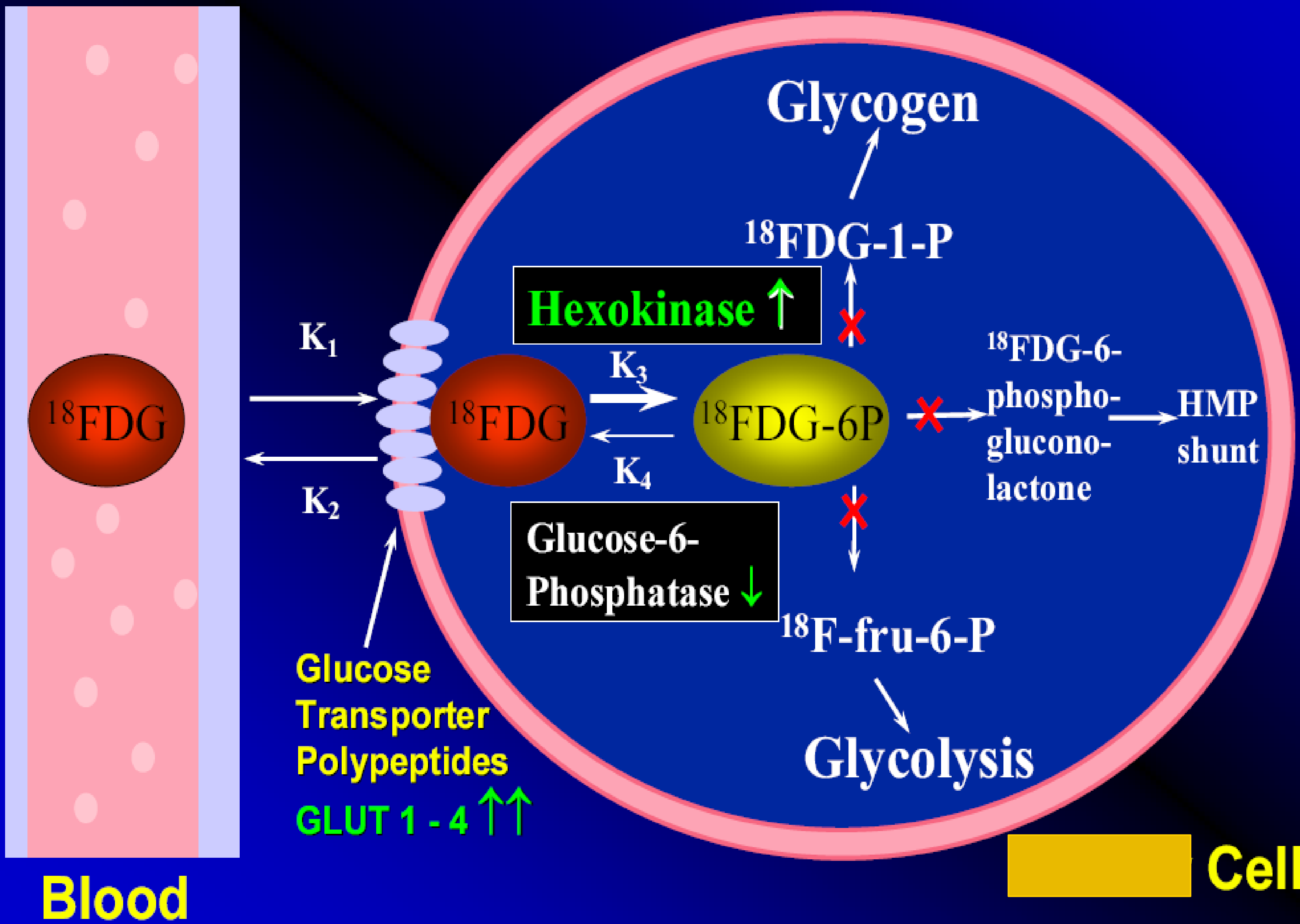

The First Brain FDG Image 1976

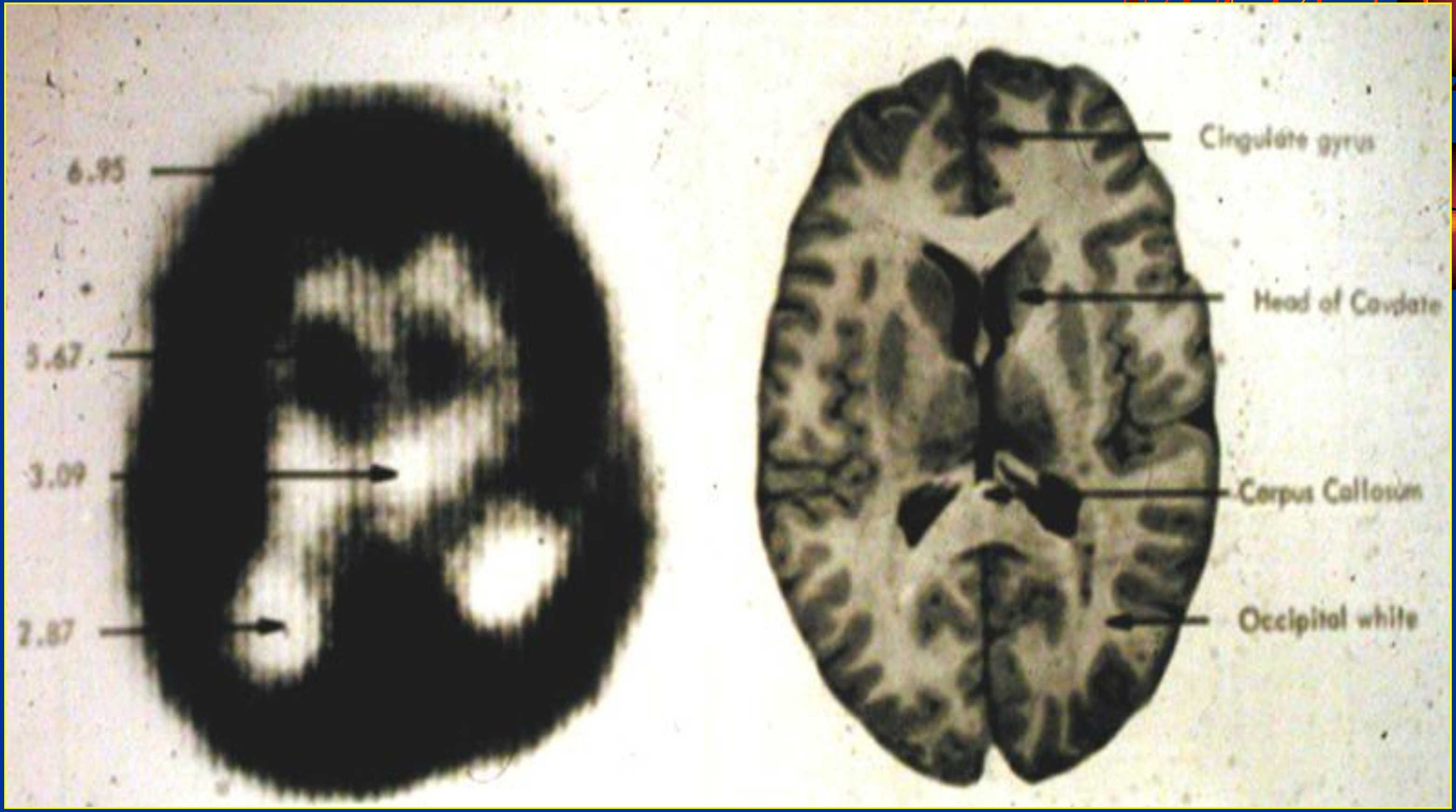

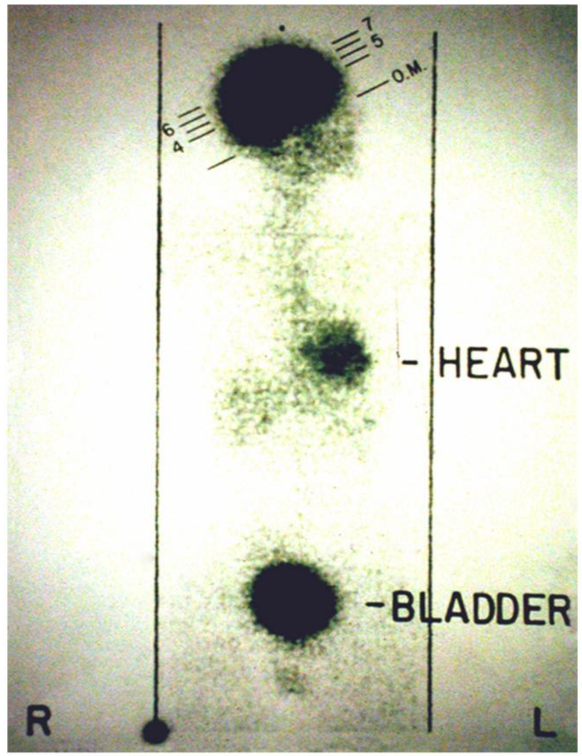

The first whole body human FDG scan was performed by
Abass Alavi
in August 1976 at University of Pennsylvania by employing a conventional rectilinear machine as the only option at the time.

Relative Sensitivity of Molecular Imaging Modalities

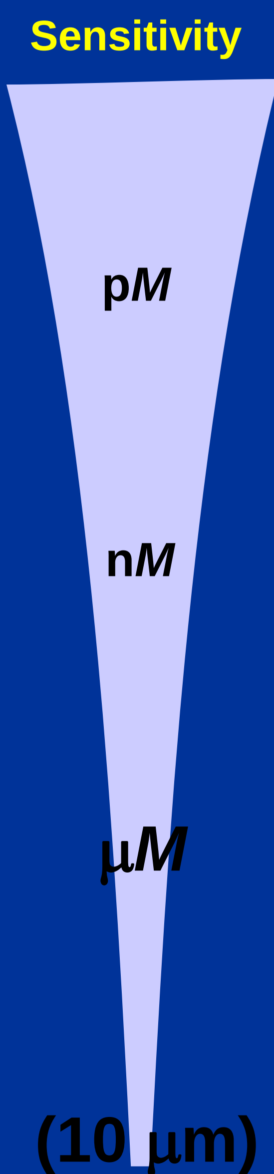

Modality	Agents	H	R	Primary uses	Examples
FMT	fluorescent proteins		X	gene expression, tagging superficial structures	GFP, RFP, NIRF probes
BLI	luciferin		X	gene expression, therapeutic monitoring	fLuc rLuc
SPECT	^{99m}Tc, $^{123/5}$I, ^{111}In	X	X	site-selectivity, protein labeling	^{99m}Tc-annex in V, ^{123}I-A85380
PET	^{11}C, ^{18}F, ^{124}I, $^{64/62/60}$Cu	X	X	site-selectivity, gene expression, drug development	^{11}C-RAC, ^{124}I-FIAU, ^{64}Cu-ATSM
spectro-scopy	endogenous metabolites	X	X	CNS, prostate , heart , breast	NAA, Cr, Cho, Glx, ml, ^{31}P
contrast agents	Gd, Mn, FeO		X	cell trafficking, enzymatic activation	poly-L-lysine, dendrimers, MION
contrast agents	perfluorinated microbubbles		X	drug-delivery, gene transfection	human albumin (Optison)

Integrated PET-CT Systems

Siemens

GE

Philips

Current and Potential Indications for FDG-PET Imaging

- CNS Disorders (AD, Seizures disorders)
- Cancer
- Infection
- Inflammation
- Myocardial Viability
- Atherosclerosis
- Muscle Dysfunction
- Clot detection

Normal Variation and Effects of Aging on Organ Function and Structure as Demonstrated by Modern Imaging Modalities

Abass Alavi, M.D.

M.D.(Hon),Ph.D.(Hon), D.Sc.(Hon)

University of Pennsylvania School of Medicine

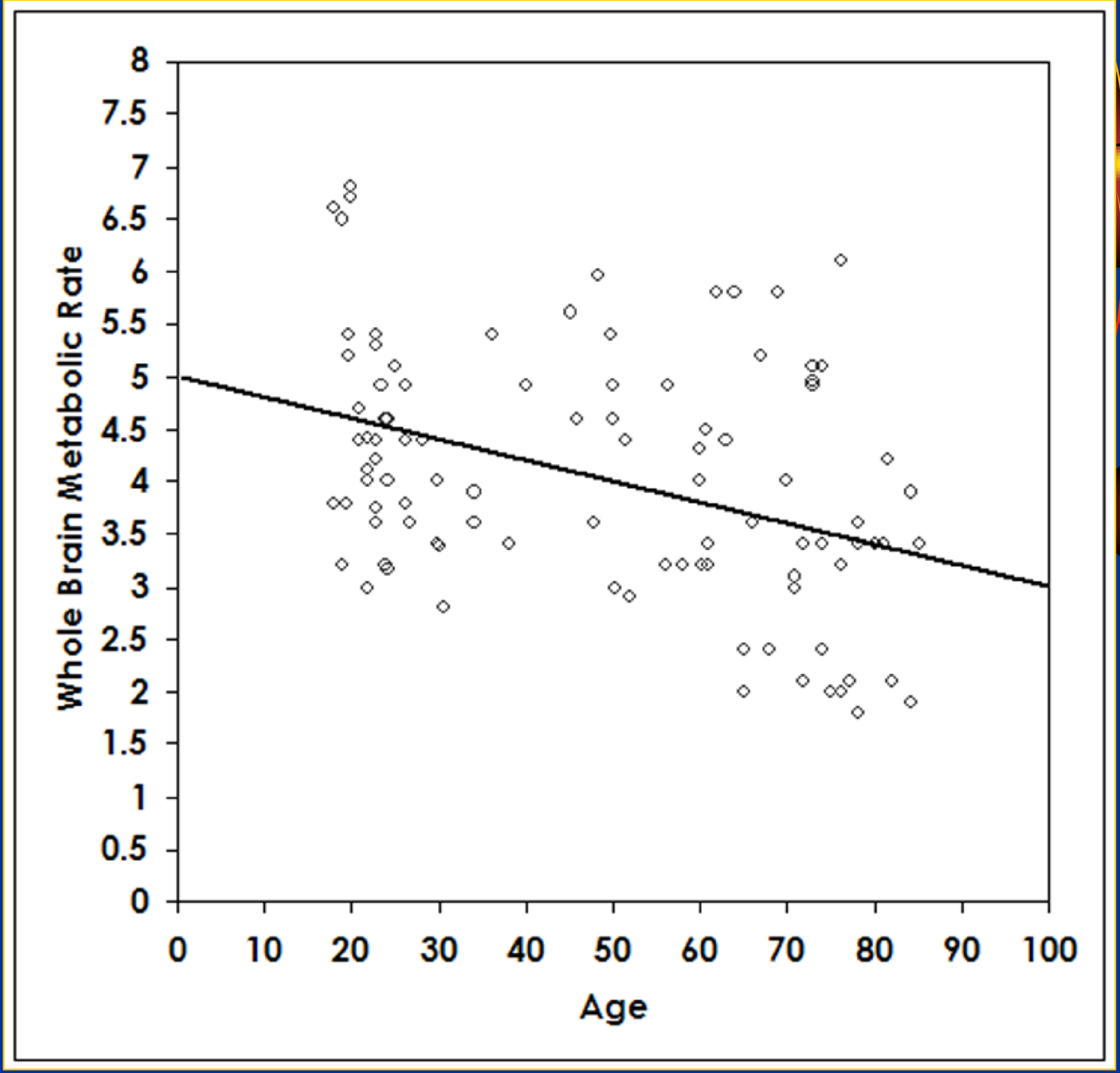

Correlation between age and whole brain metabolic rate (age range: 18– 85 years).

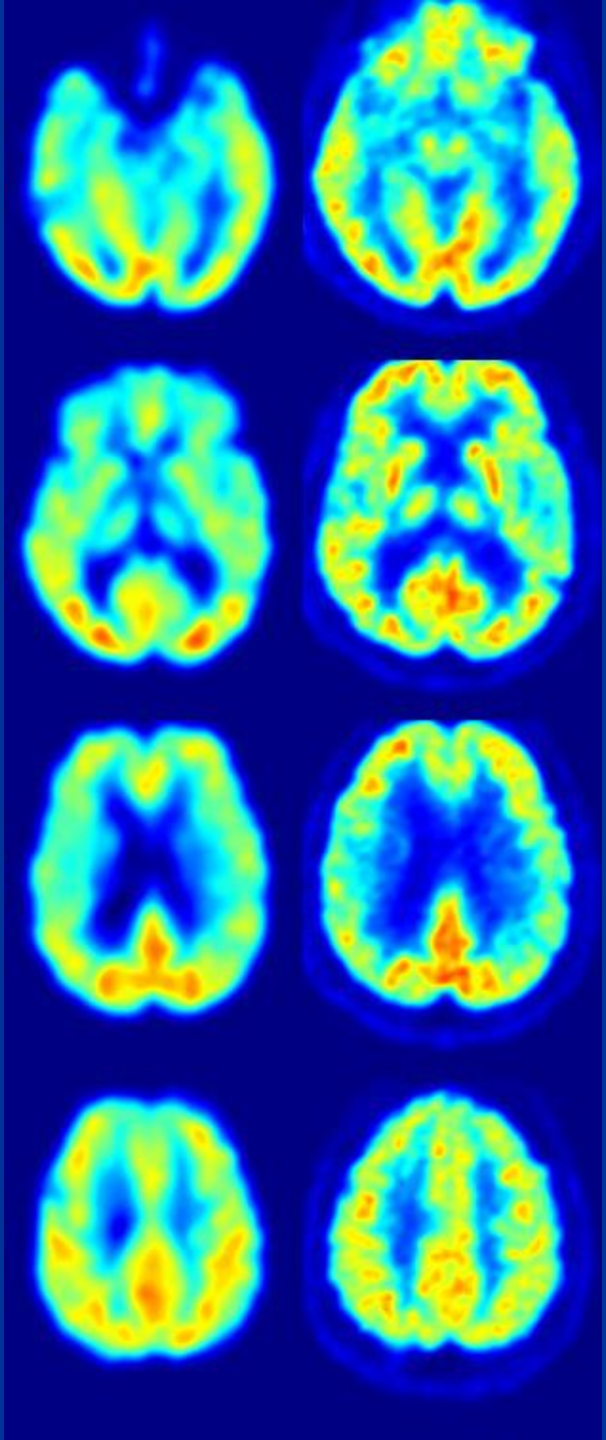
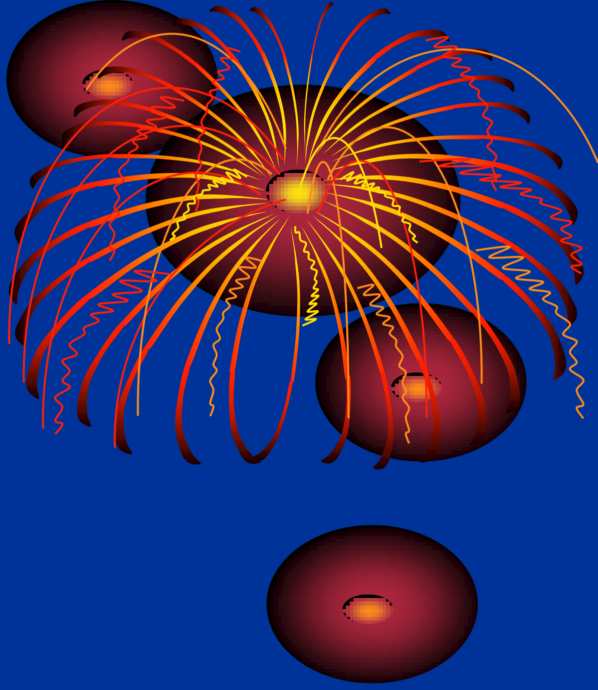

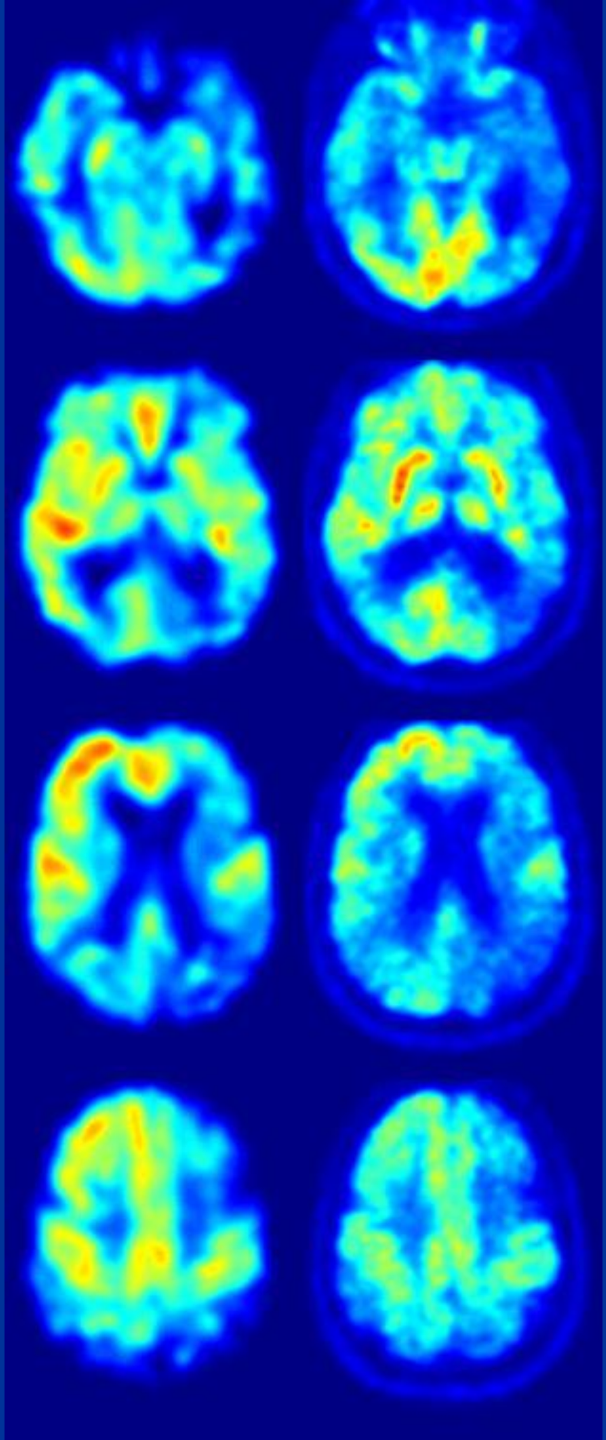

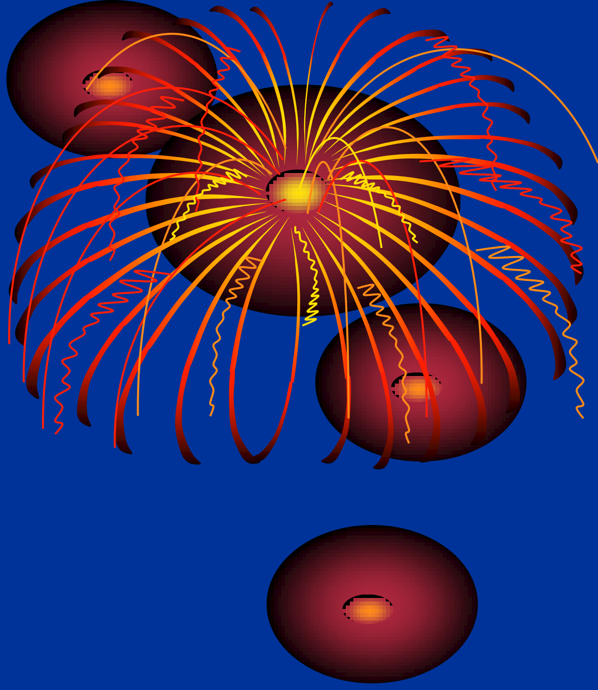

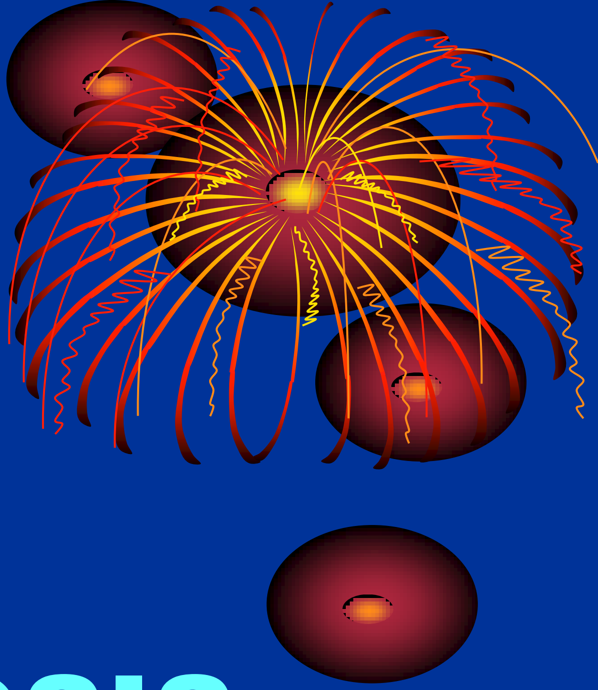

- **CANCER DIAGNOSIS**

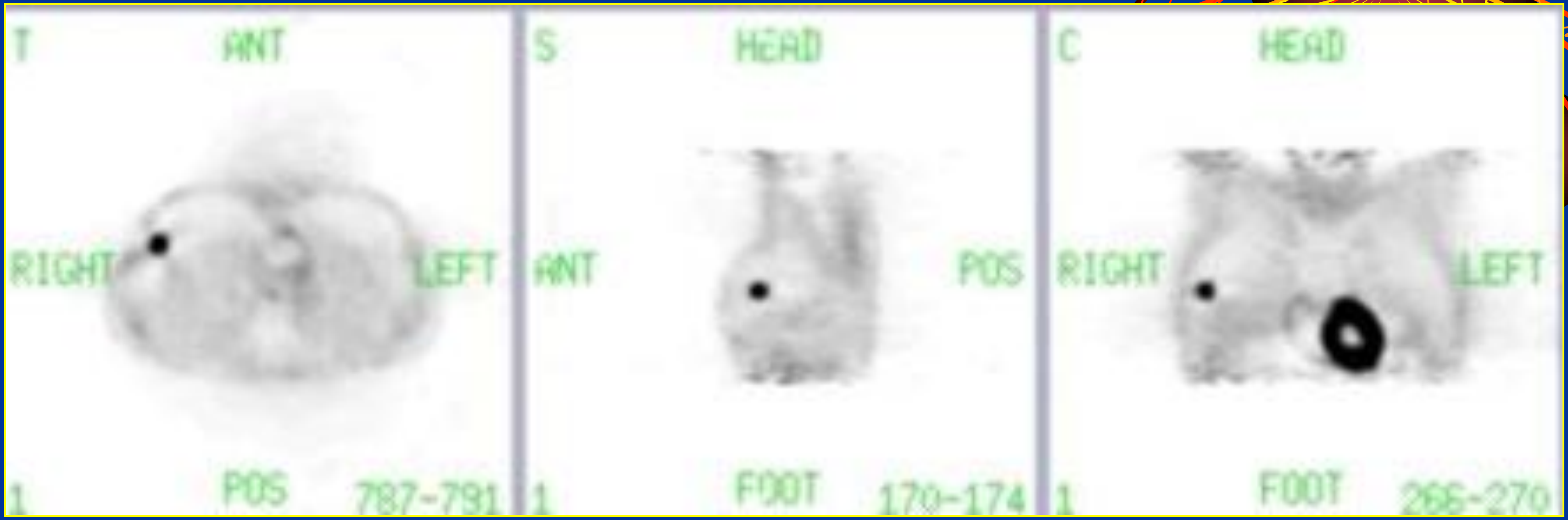

58 yrs old female with Palpable mass in Right Breast

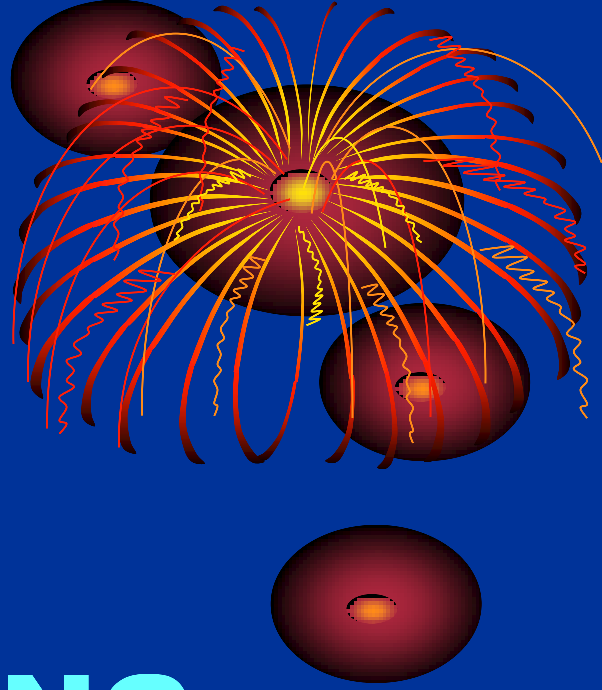

- **CANCER SATAGING**

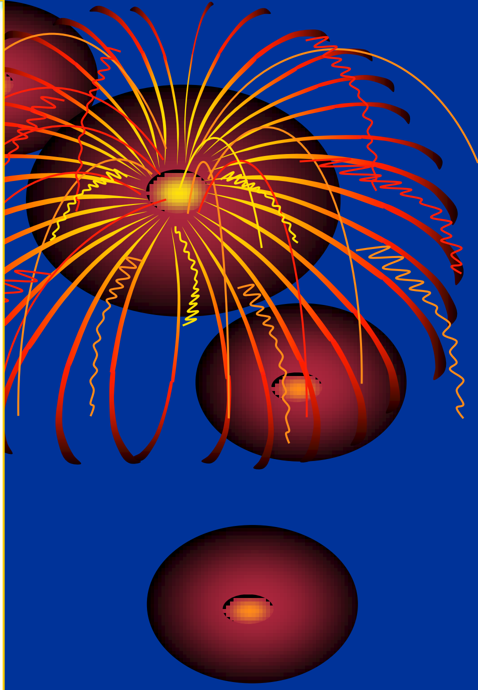

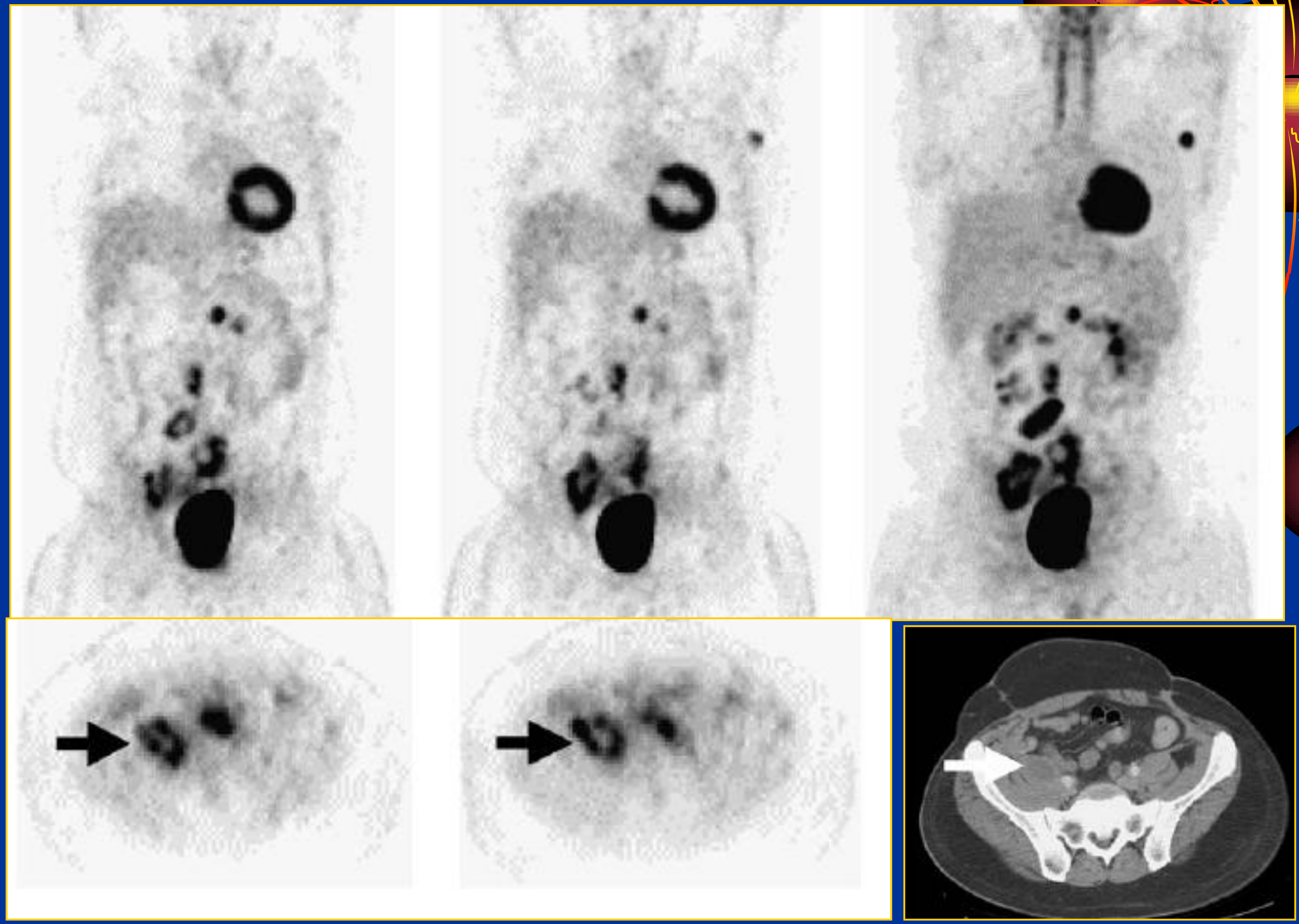

Staging widespread melanoma

- **ASSESSING RESPONSE TO THERAPY**

Early Assessment for Response

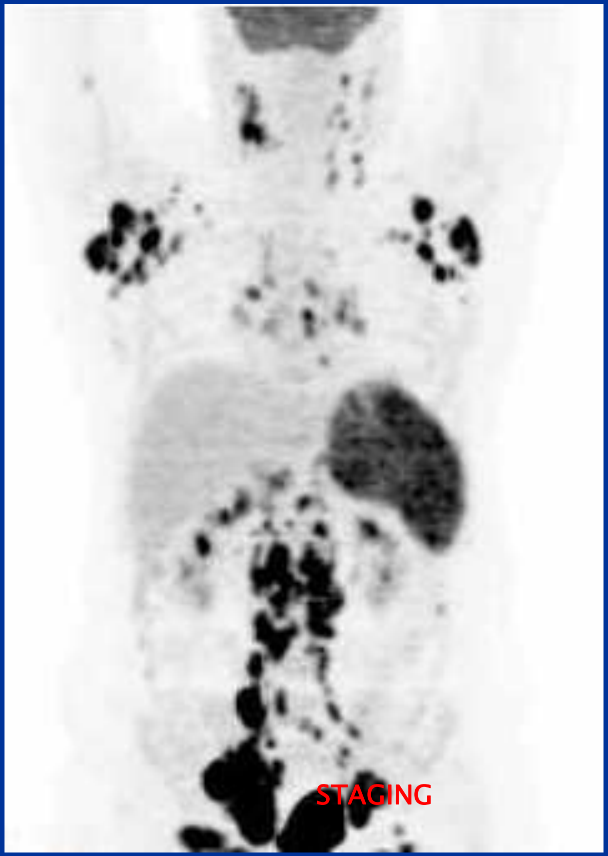

CT BASED PRACTICE

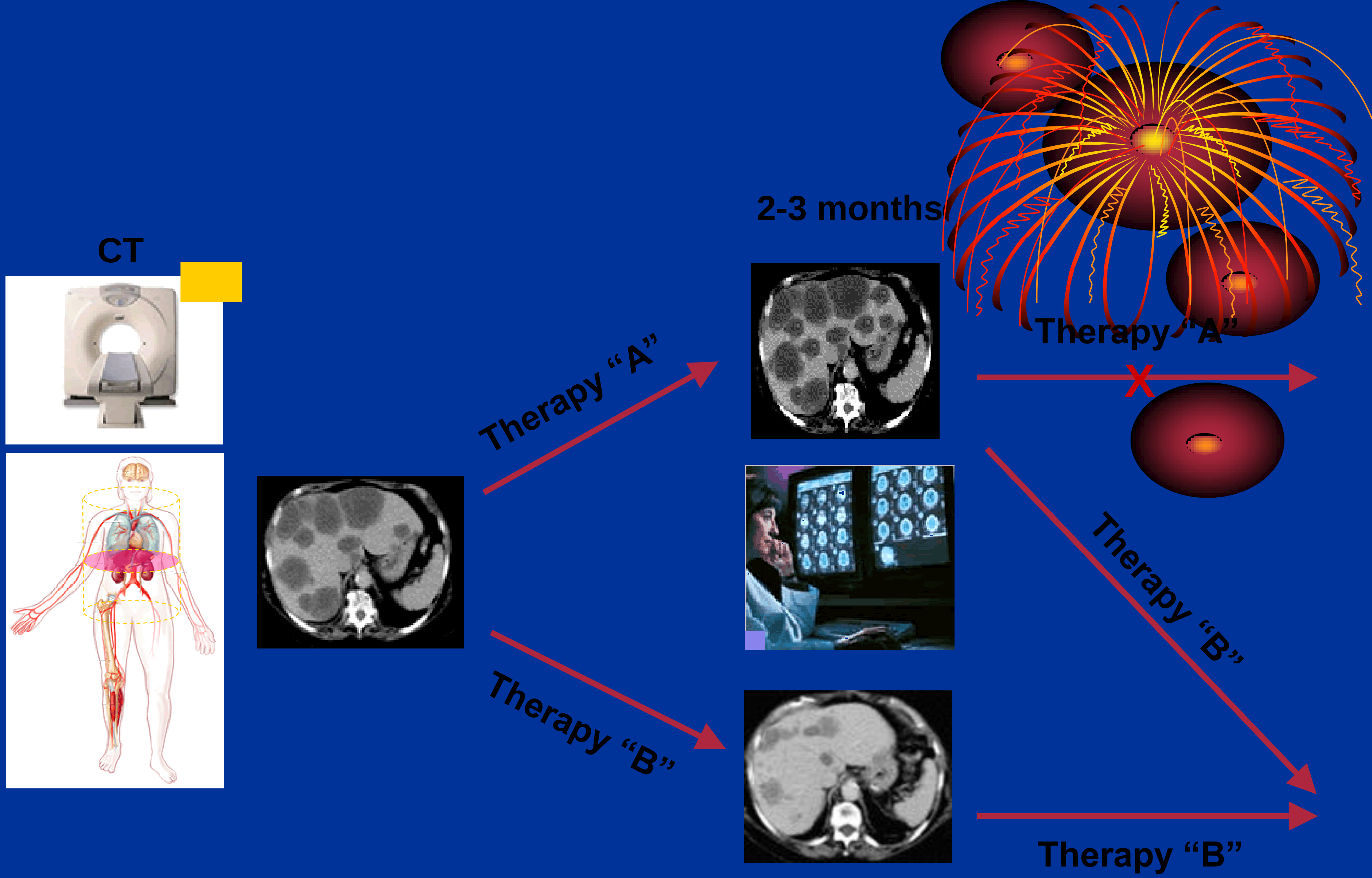
CT
Therapy “A”
Therapy “B”
2-3 months
Therapy “A”
X
Therapy “B”
Therapy “B”

- **PET BASED PRACTICE**

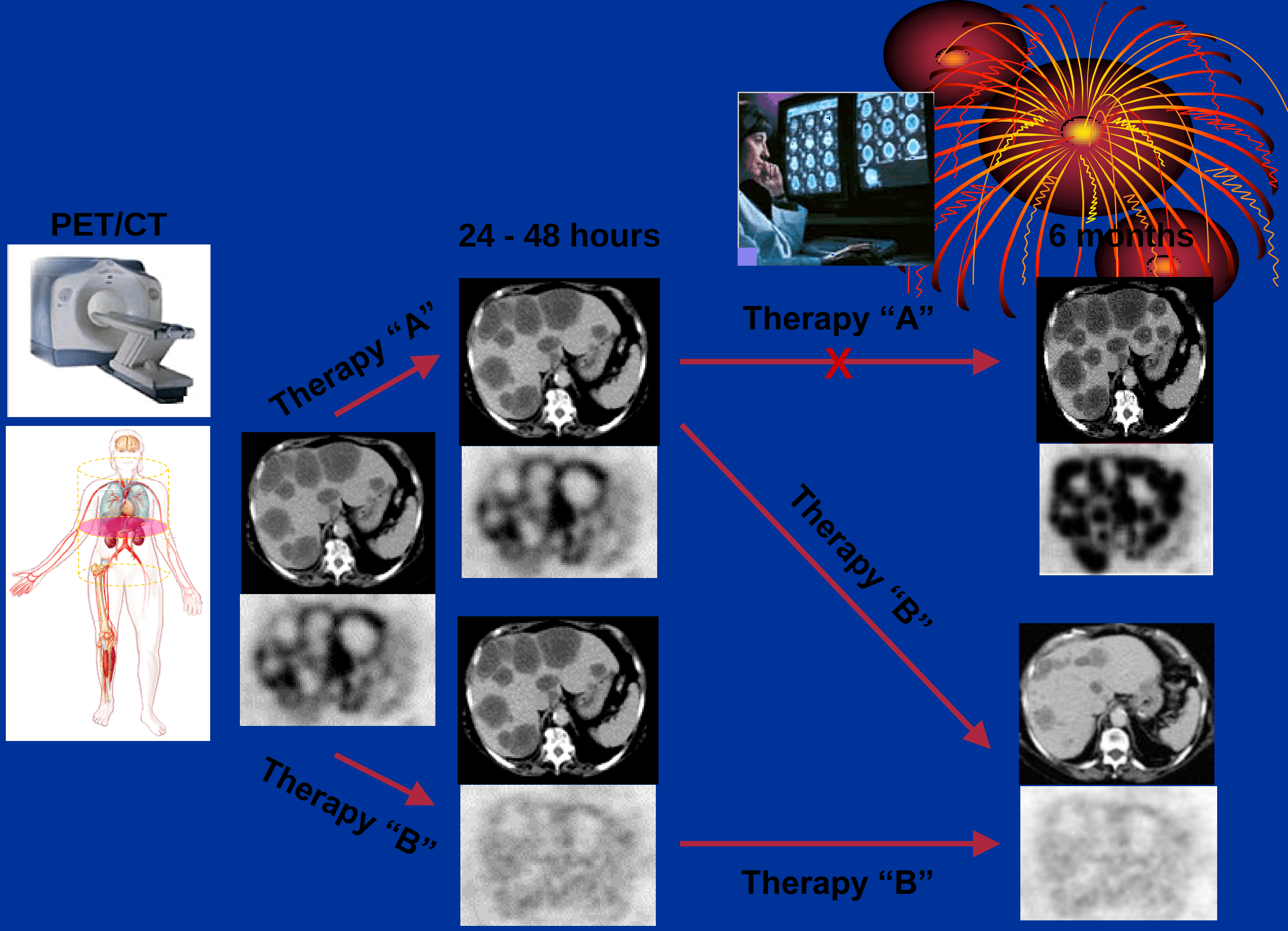
PET/CT
24 - 48 hours
6 months
Therapy "A"
Therapy "B"
Therapy "A"
X
Therapy "B"
Therapy "B"

- DETECTION OF RECURRENCE

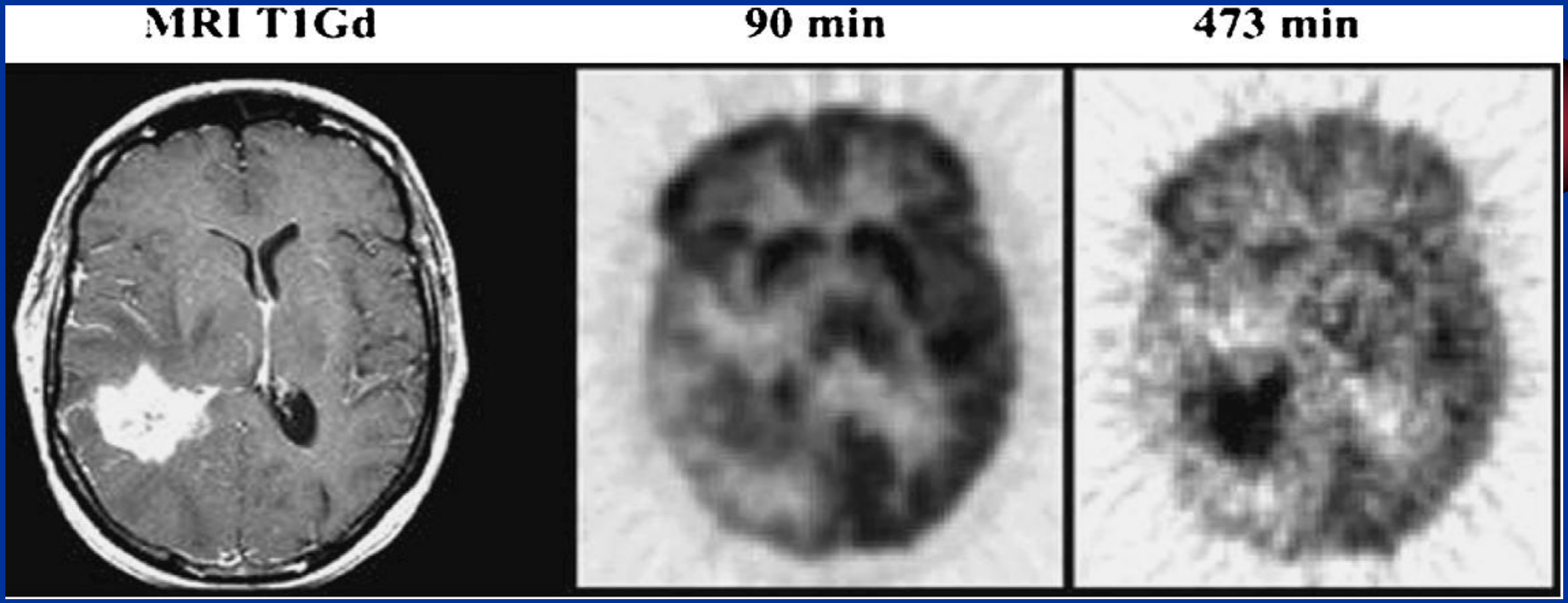
MRI T1Gd
90 min
473 min

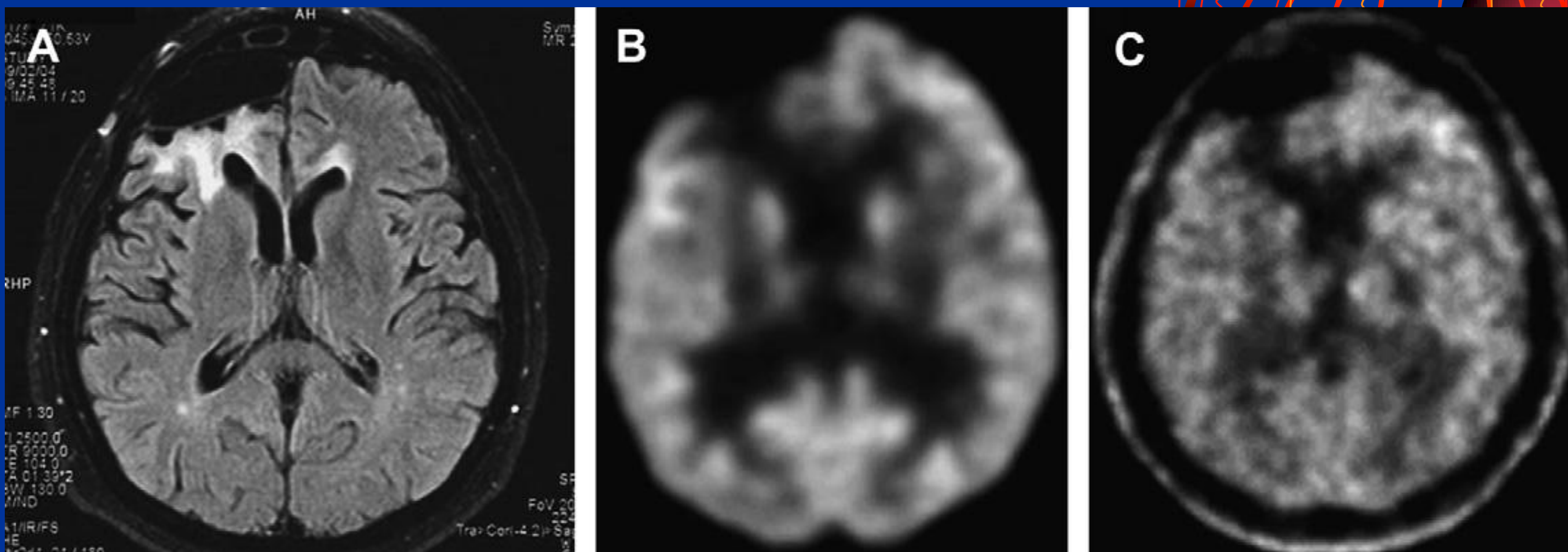
A
B
C

The Role of PET-CT/MRI Co-registration in Radiation Therapy

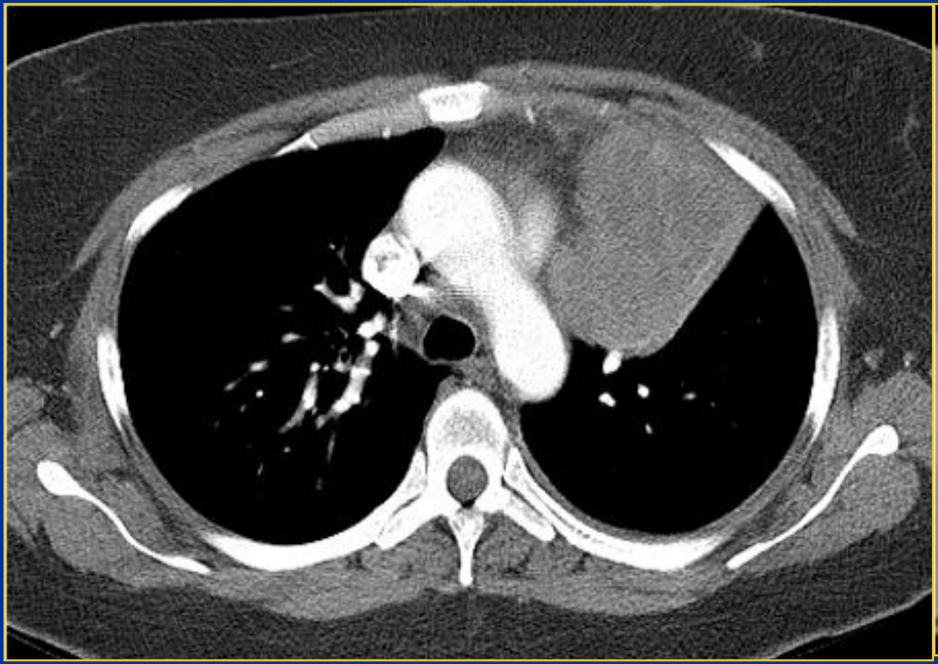

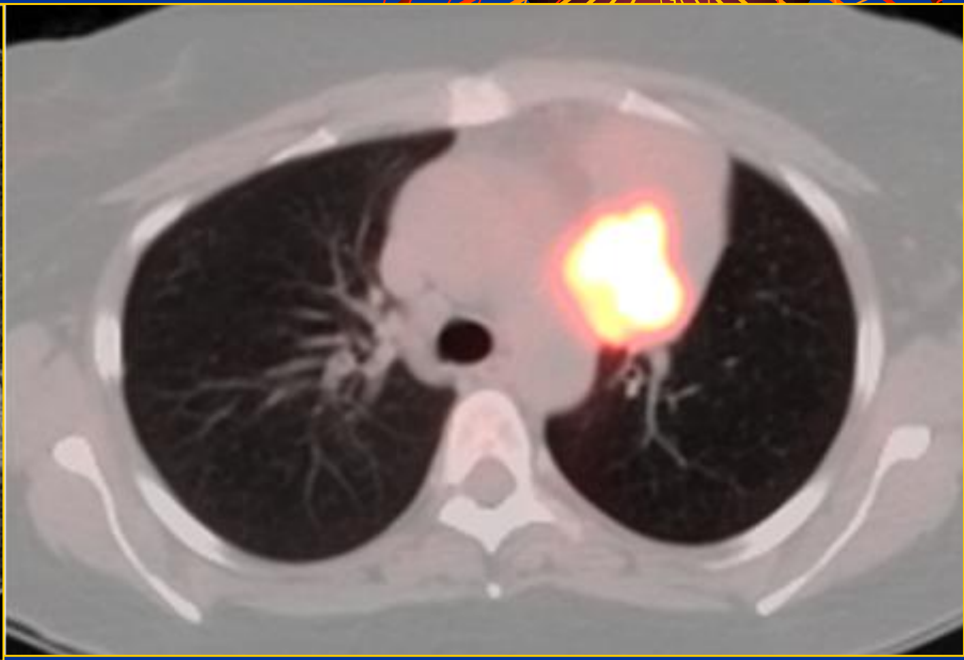

FDG-PET for the Diagnosis of Infections and inflammation

Chronic Osteomyelitis

Sinus Track Connecting Soft-Tissue Abscess With Bone

Sagittal FDG-PET	Precontrast SPGR	Postcontrast SPGR

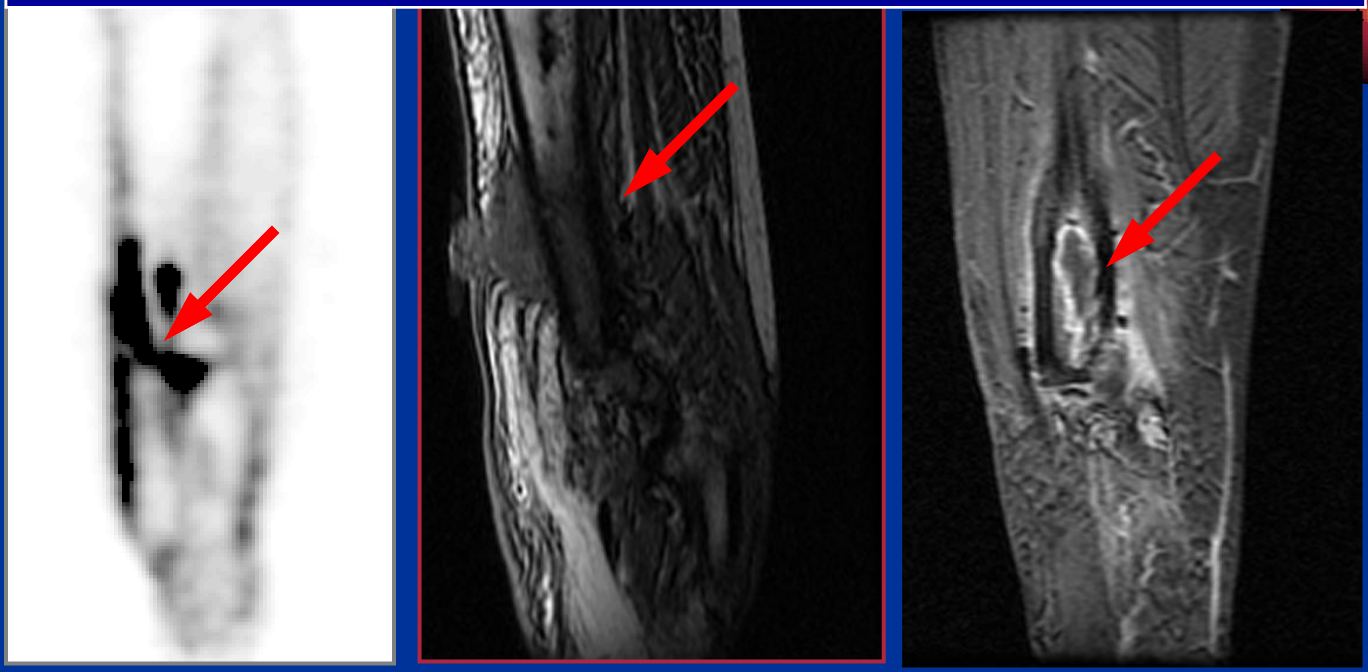

SPGR = spoiled gradient.

FDG-PET/CT in Diabetic Foot

FDG-PET Image- vasculitis is confirmed.

Otsuka H, Morita N, Yamashita K, Nishitani H.
FDG-PET/CT for diagnosis and follow-up of vasculitis.
J Med Invest. 2007 Aug;54(3-4):345-9.

Inflammatory Bowel Disease

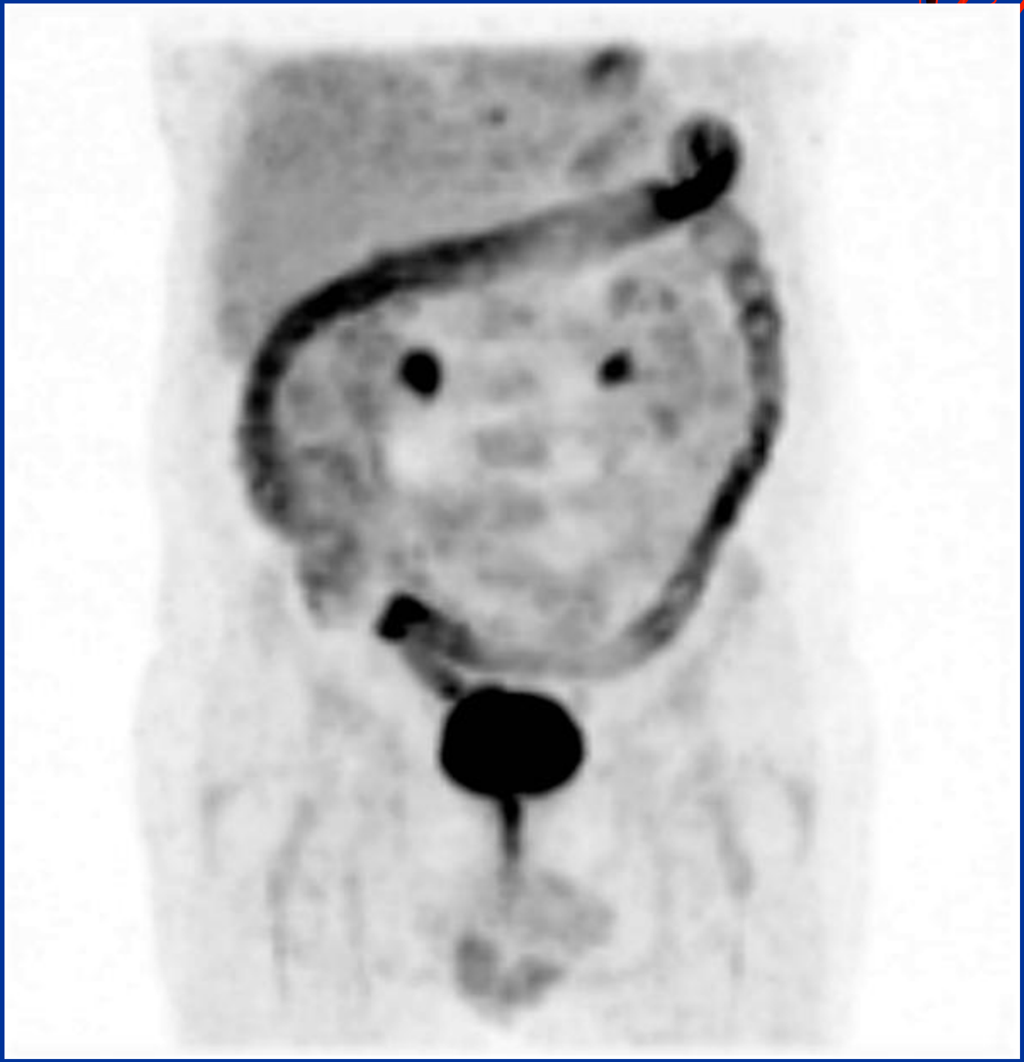

Atherosclerosis

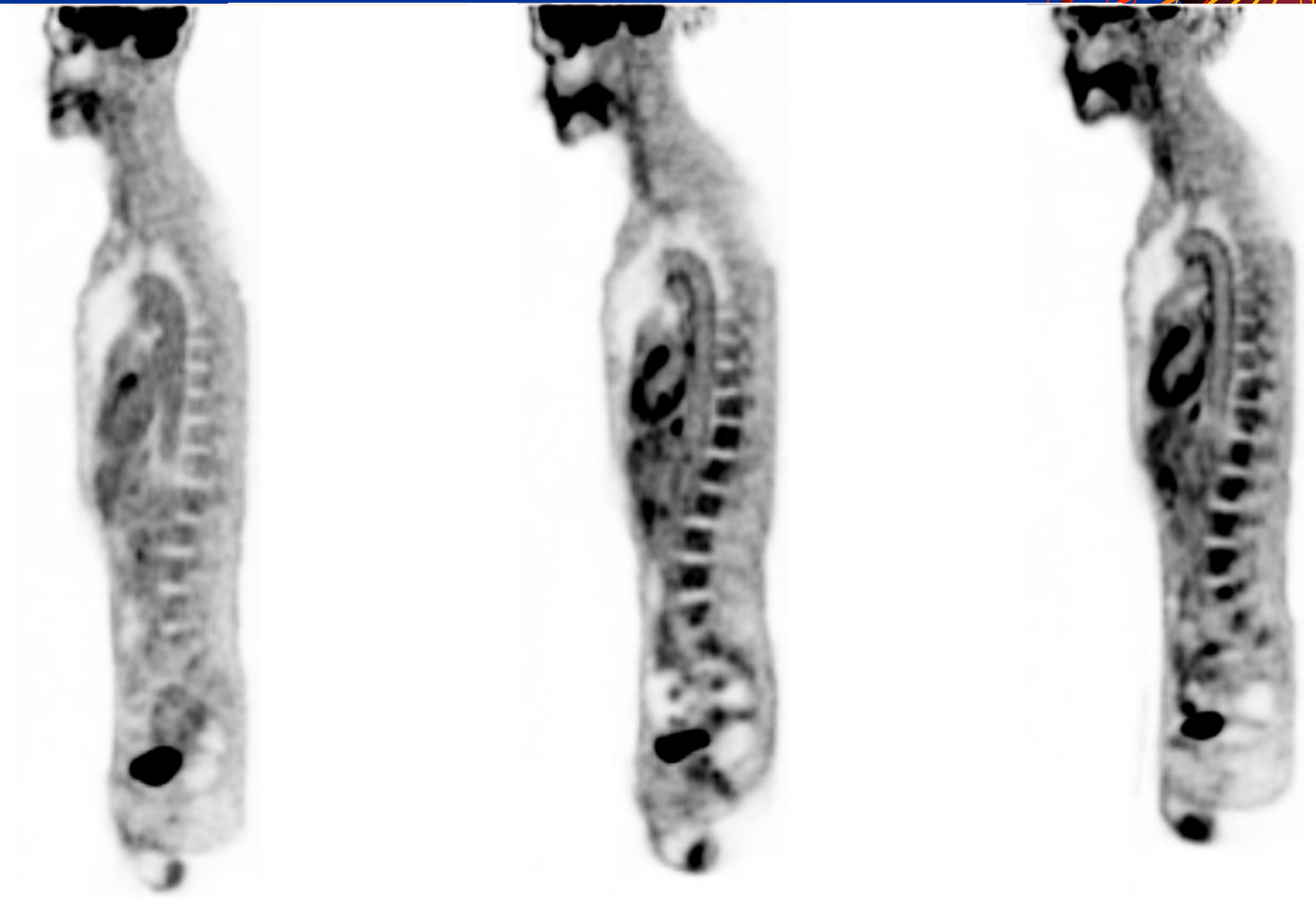

First Hour **Second Hour** **Third Hour**

FDG PET CT – Inflammation in Aorta

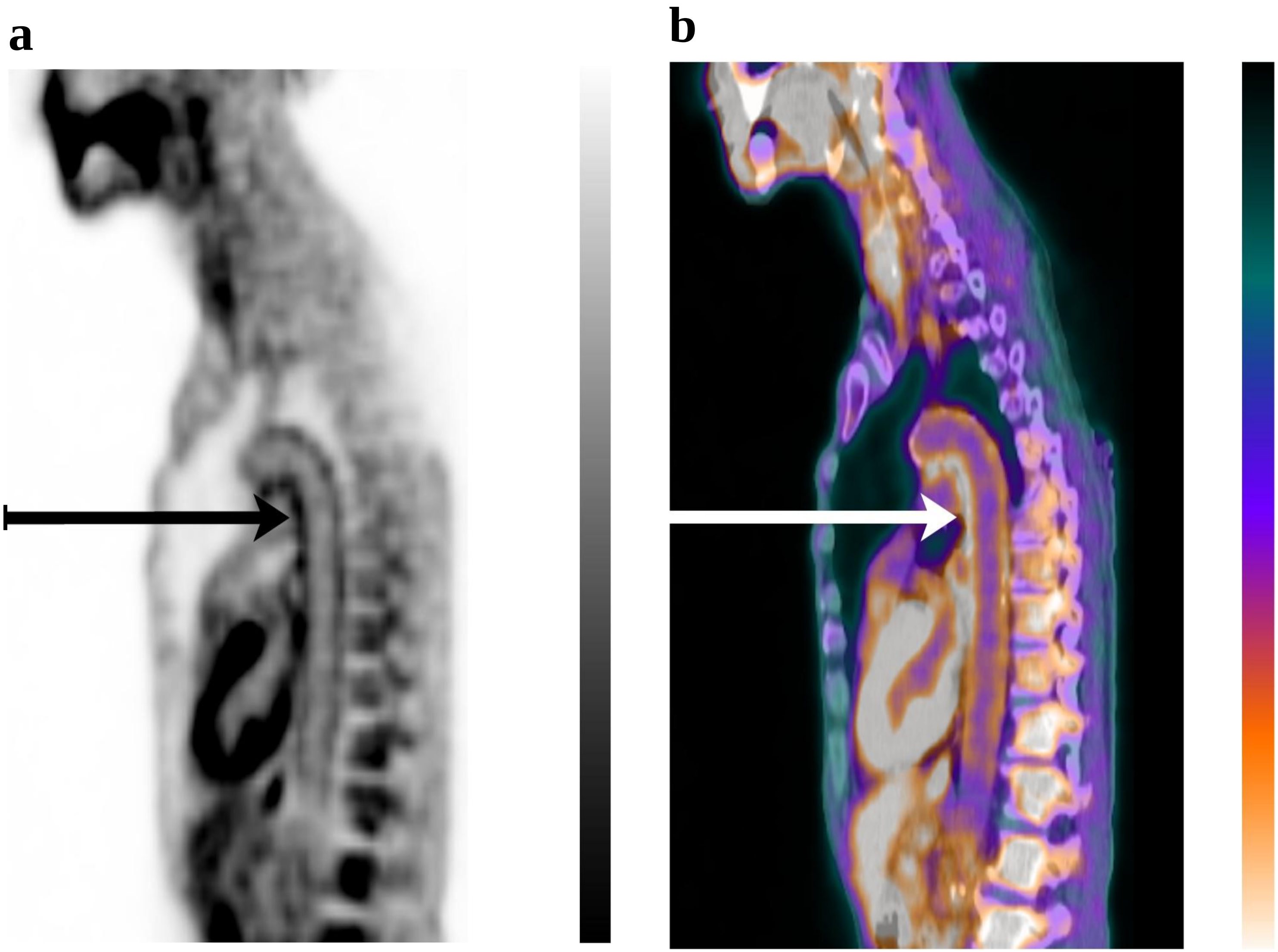

FDG PET + CT

24-year old male

60-year old female

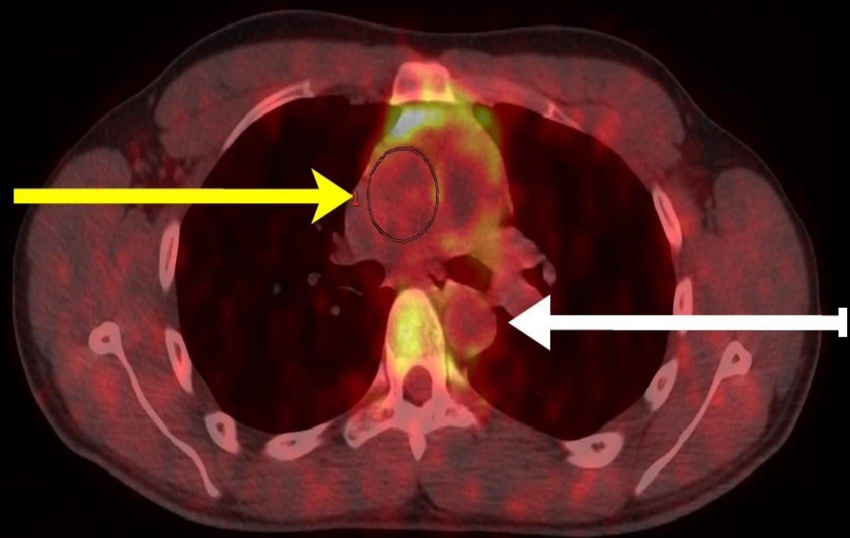

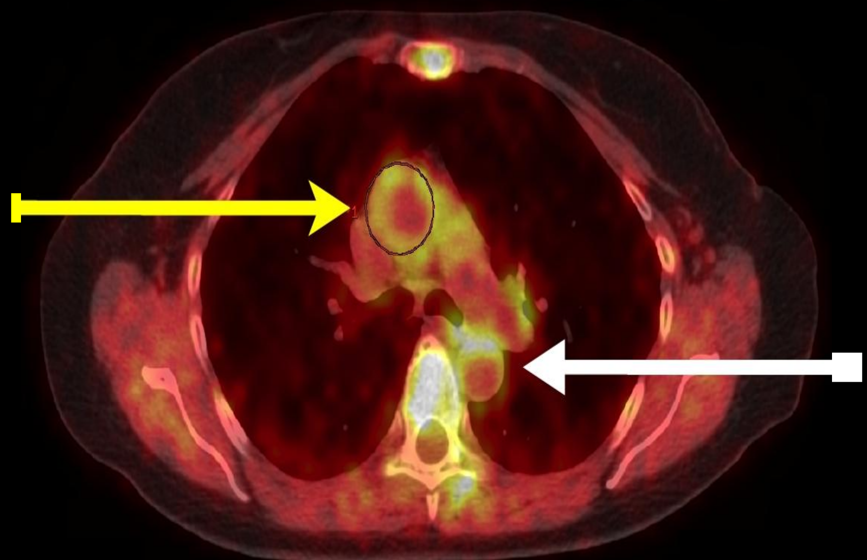

FDG PET CT

FDG PET CT

Blomberg, Høilund-Carlsen, 2012

61-year-old caucasian male

- Adipose, recent pneumonia and gout, bedridden for weeks
- 2 day history of swelling and tenderness of right lower extremity
- D-dimer 19 mg/L (ref. < 0,5 mg/L), Wells' score 4

- CUS: RLE DVT (mid-femoral to distal calf)
- PET/CT: Positive for RLE DVT, otherwise normal

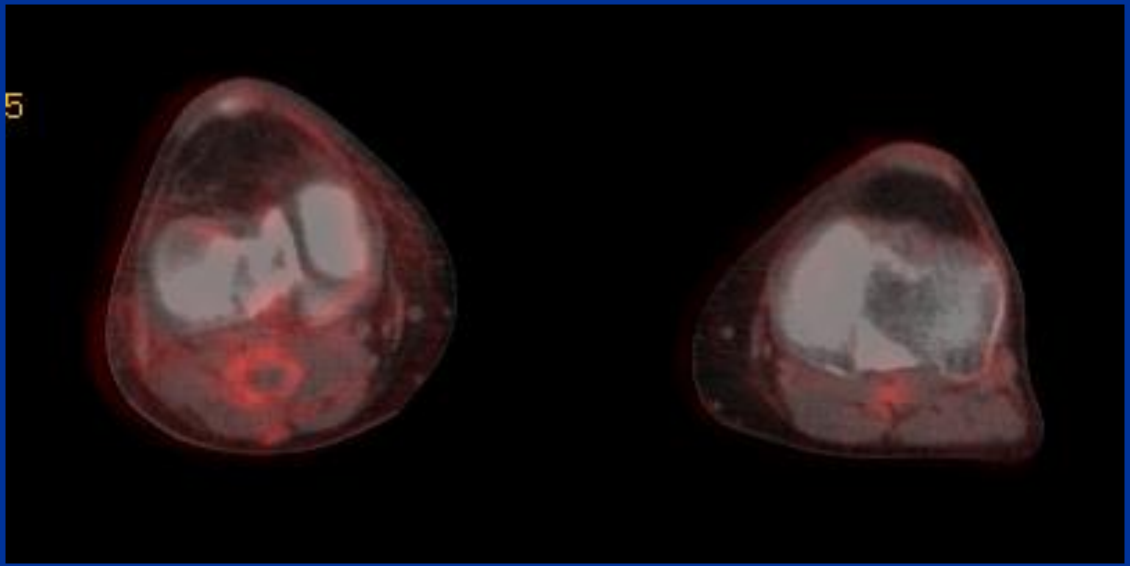

Differential dynamics of FDG between malignant and inflammatory cells

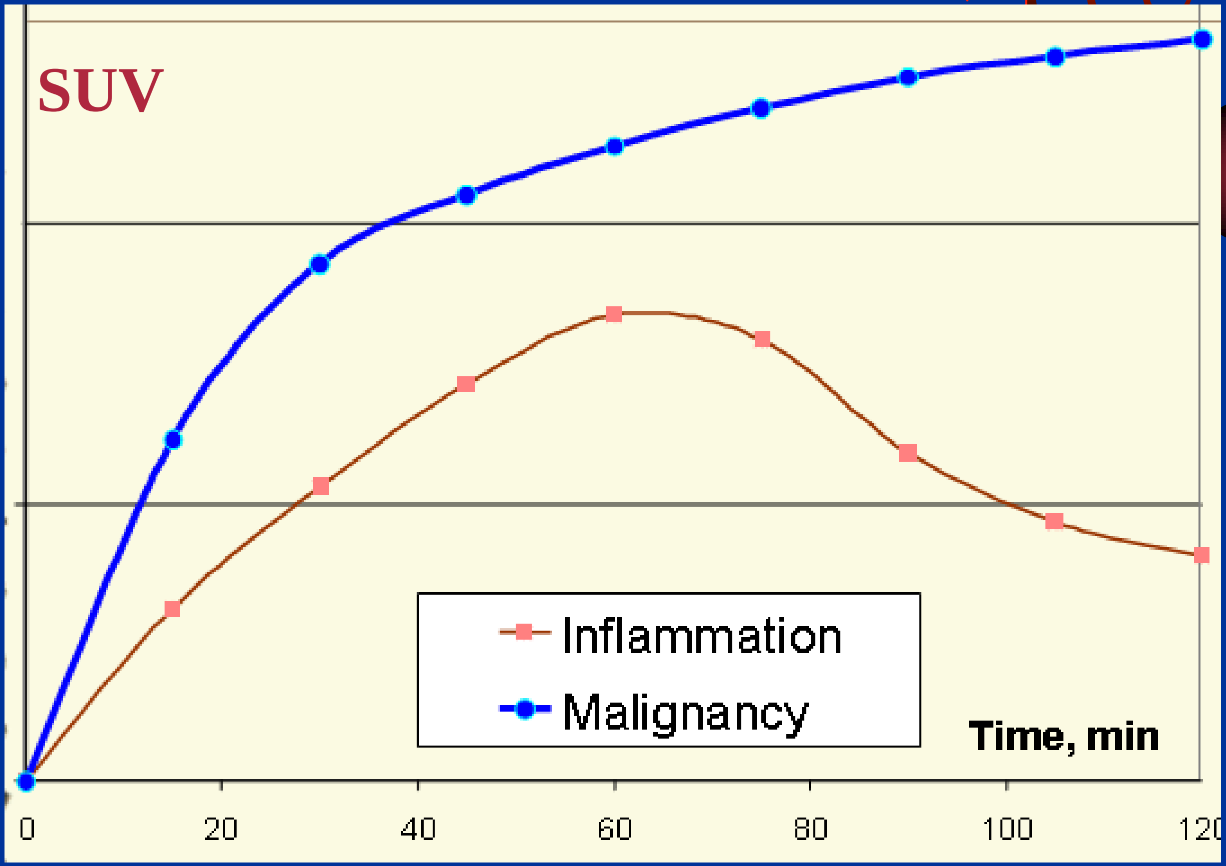

[^{18}F] FDG – the Molecule of the Century
Uptake and Metabolism

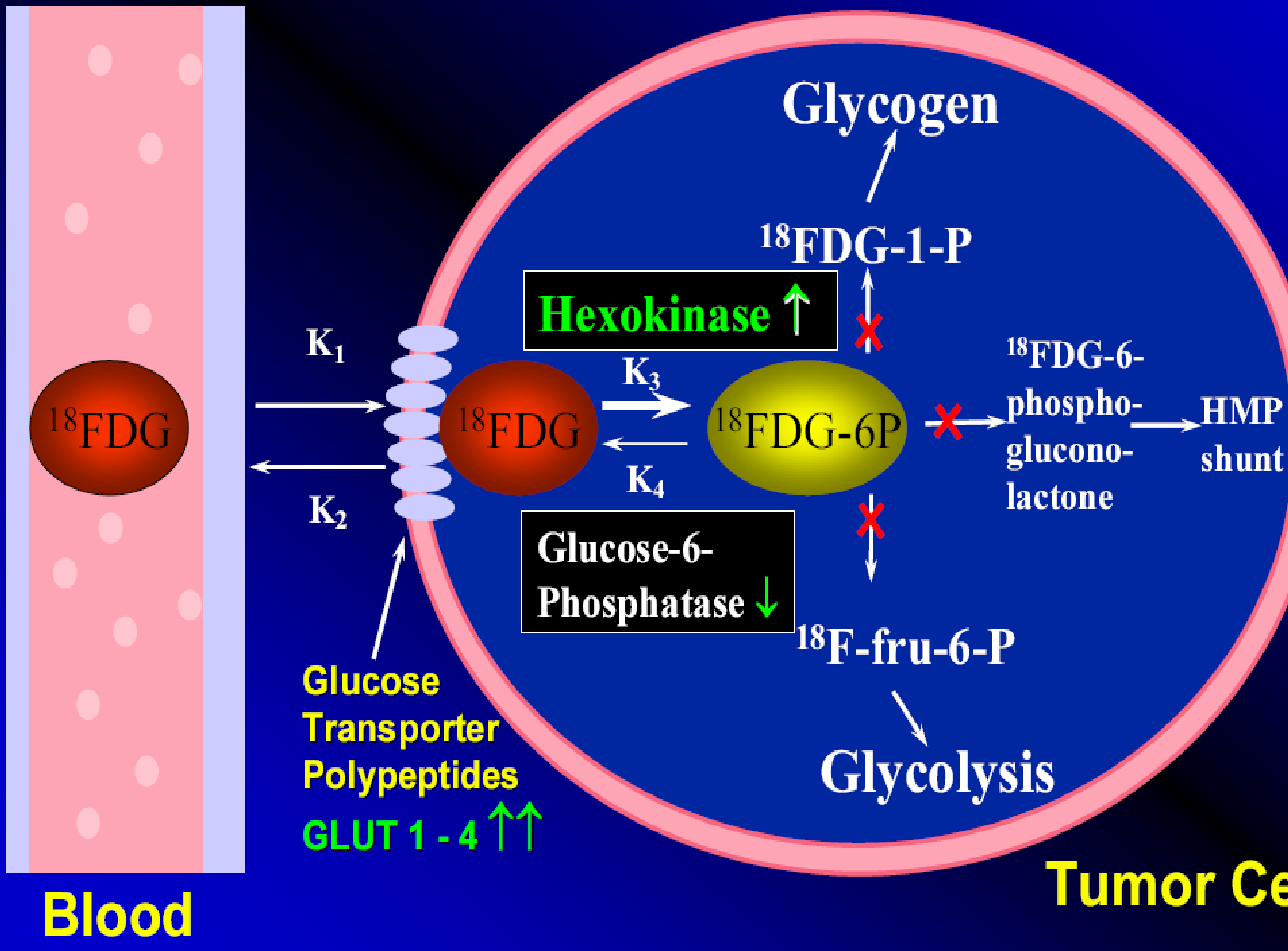

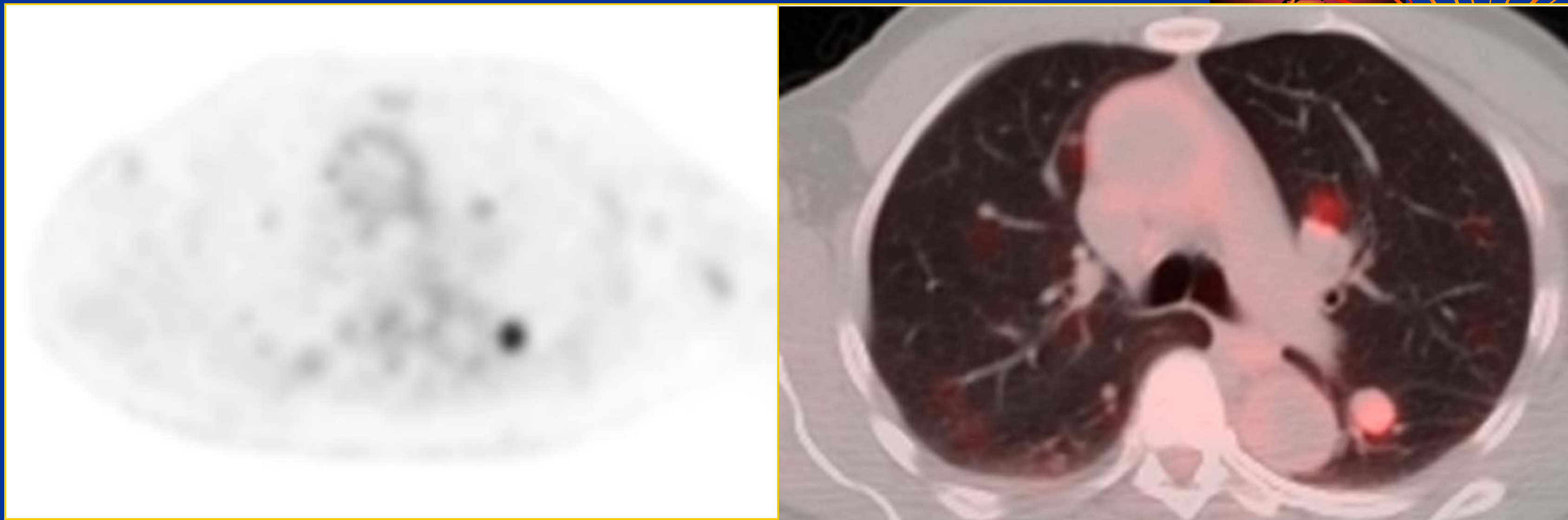

Time 1

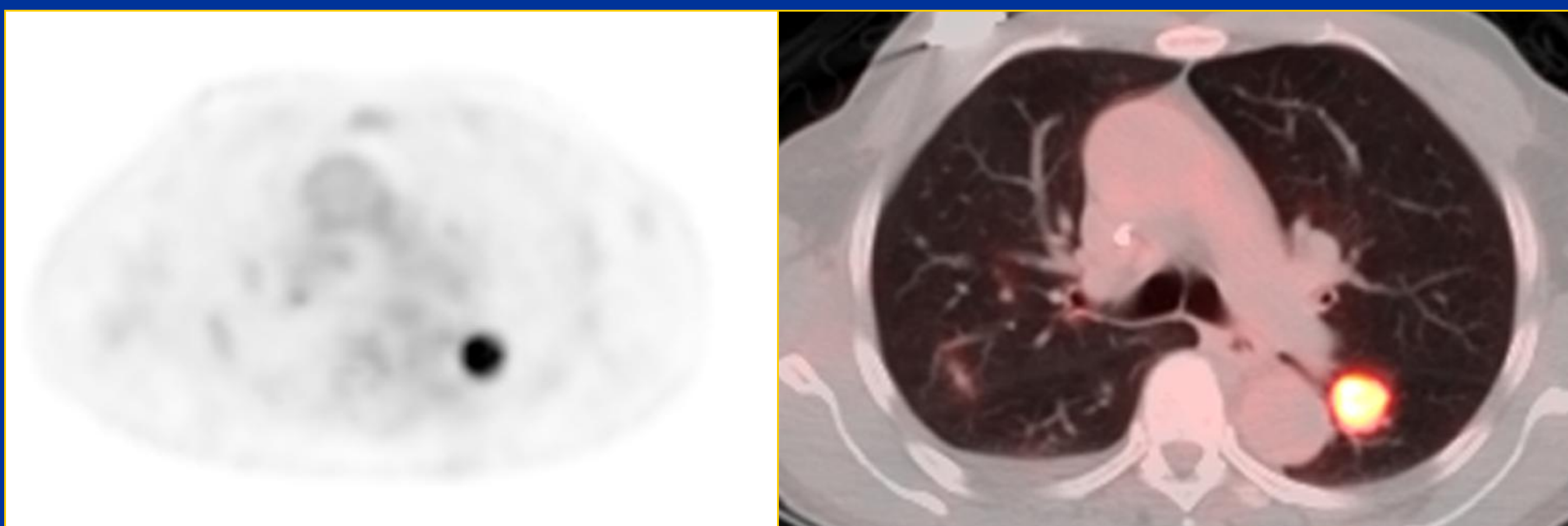

Time 2

Retention Index: SUVmean

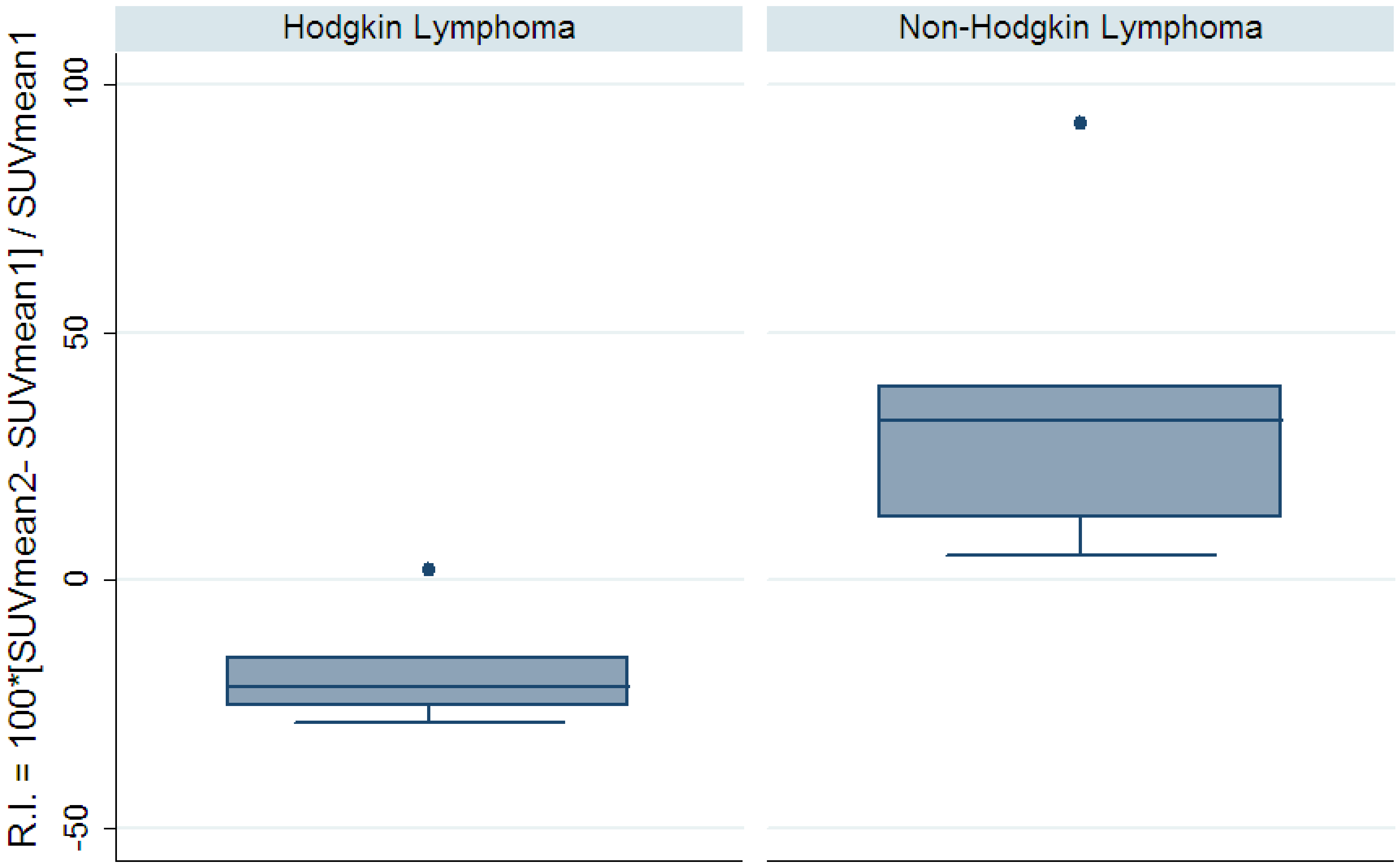

P-Value = 0.004

Lung Ca, additional pleural and Lymph nodes mets

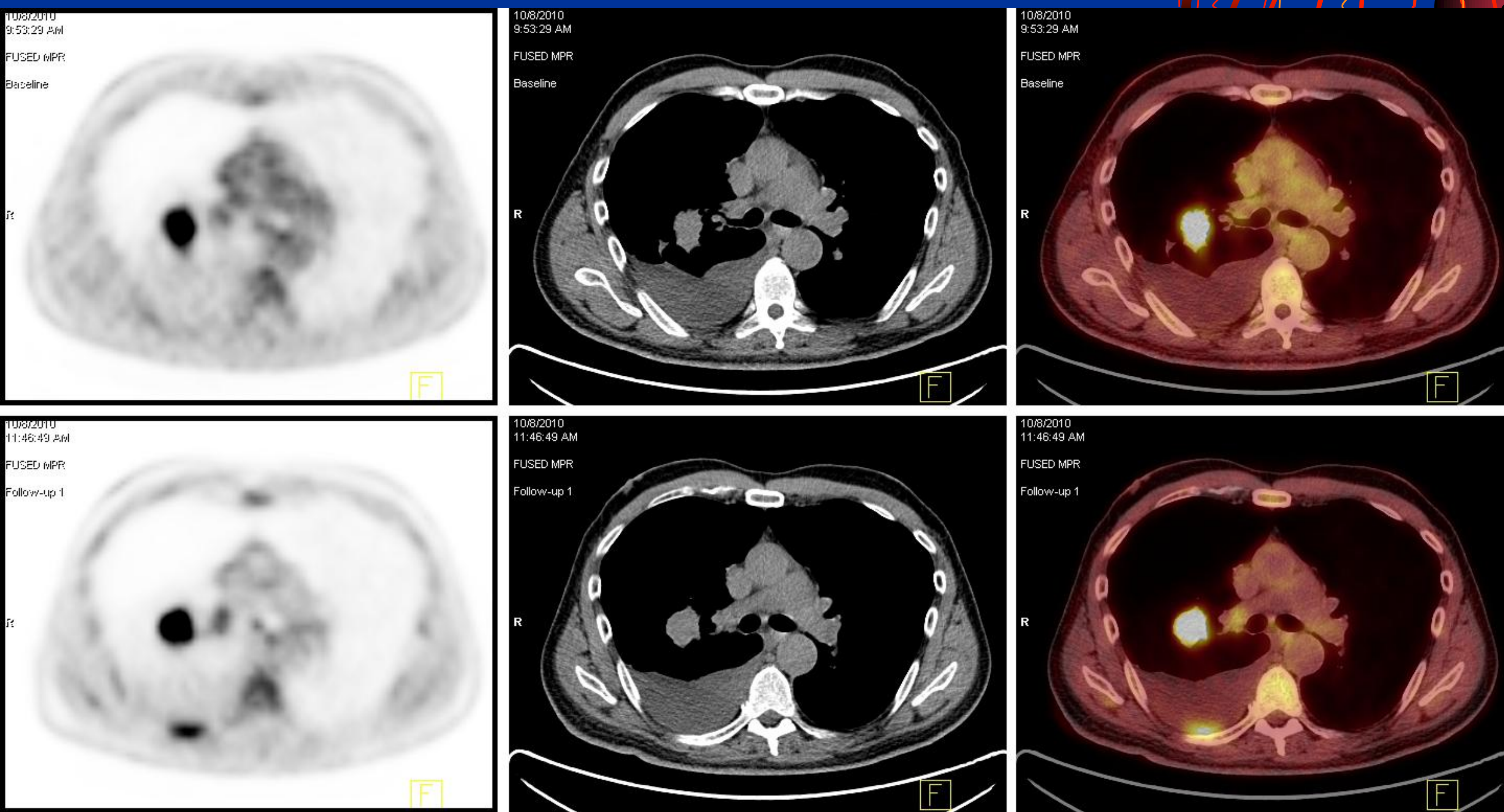

1 hour

3 hours

FIRST TIME POINT (Early)

SECOND TIME POINT (Delay)

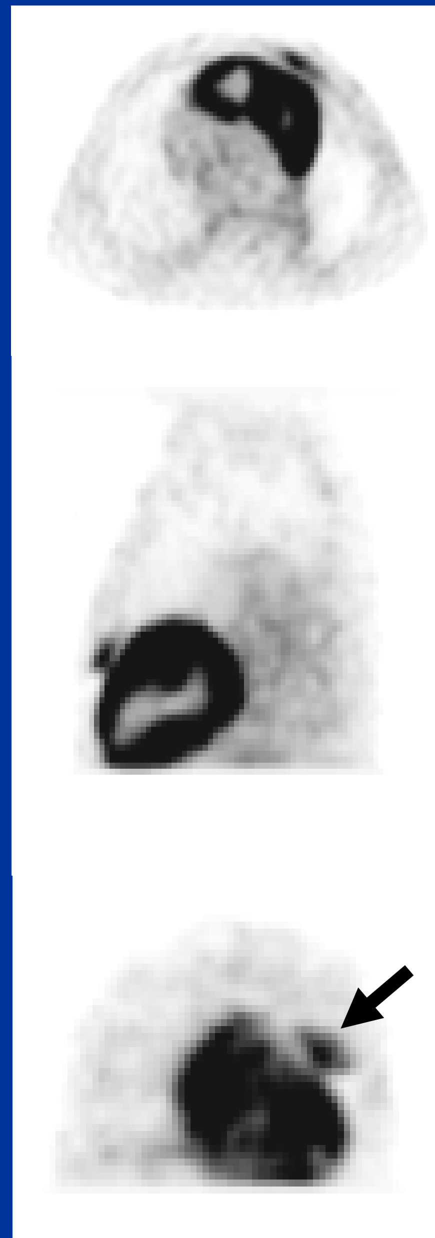

DUAL TIME IMAGING IN MESOTHELIOMA

Early Image Max SUV= 3.5

Delayed Image Max SUV= 4.8

RESULTS

Table

Histopathology	Avg. SUVmax 1	Avg. SUVmax 2	Avg. Percent SUV Change (%)
Malignant Mesothelioma (n = 28)	4.6 ±2.5	5.3 ±2.8	14.0 ±12.4
Benign Pleural Disease (n = 4)	1.5 ±0.2	1.3±0.2	-10.5 ±21.6

P < 0.002

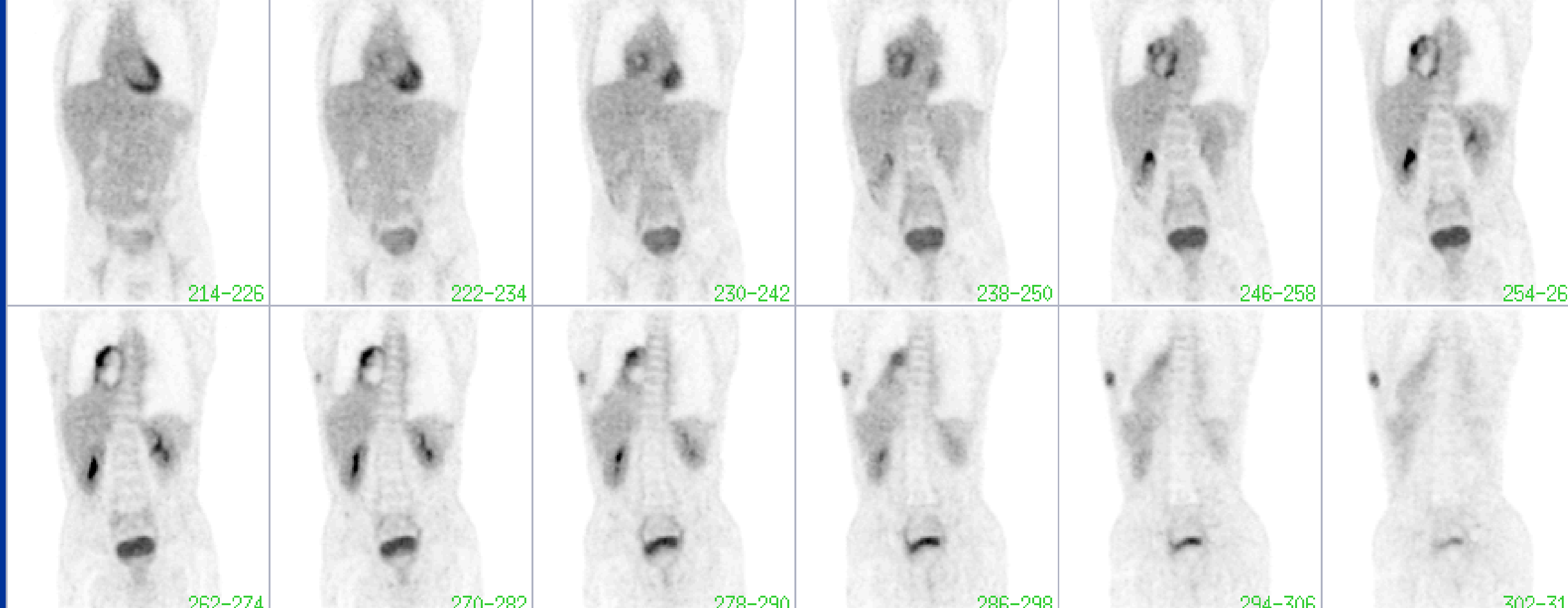

45-Minutes

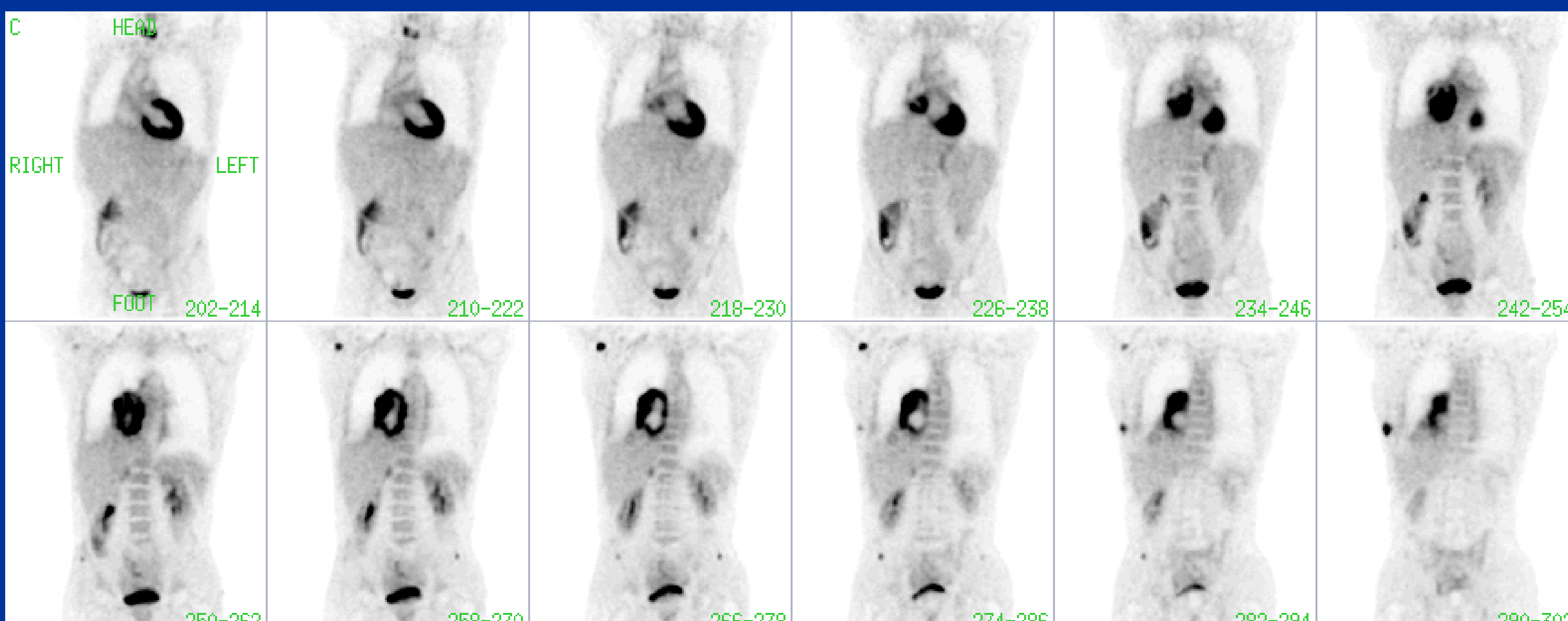

3-hour

Temporal profile of FDG uptake in Lung Cancer

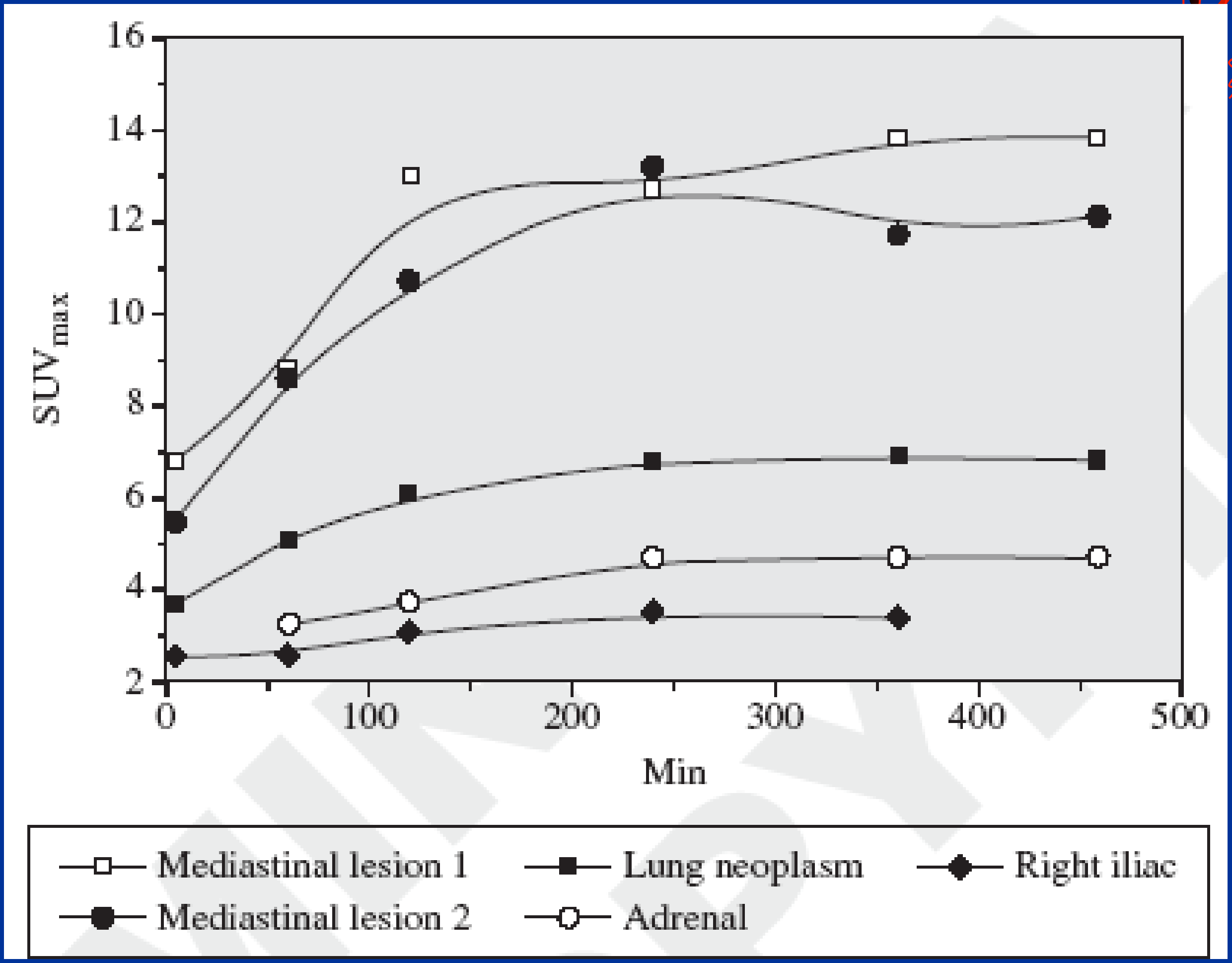

Basu S et al, QJNM 2008

Assessing Tumor Biology and Forecasting Prognosis

Assessment of Tumor Biology in Breast Cancer

Based on Time Course of FDG in the Primary Site

	Primary Breast lesions in patients without Axillary or Distant Metastasis	Primary Breast lesions in patients with Axillary Metastasis	Primary Breast lesions in Patients with Distant Metastasis	p
SUVmax1	2.9 ± 2.7	4.8 ± 3.9	7.7 ± 6.2	0.01*
SUVmax2	3.4 ± 2.4	5.3 ± 4.5	8.9 ± 7.1	0.01*
%ΔSUVmax	4.5 ± 4.2%	9.4 ± 12.8%	15.7 ± 10.8%	>0.05

SUVs in the primary lesions were highest in Gp II (those with both axillary and distant metastases), followed by Gp I (those with only metastatic axillary adenopathy) and Gp III (patients without any metastasis)

Global metabolic activity (GMA)

DLBCL

V = 306.25 cc

MVP = 5175.79 SUV cc

cMVP = 9333.10 SUV cc

Δ MVP = 80.3%

Torigian DA et al, unpublished data DLBCL

Life Beyond FDG

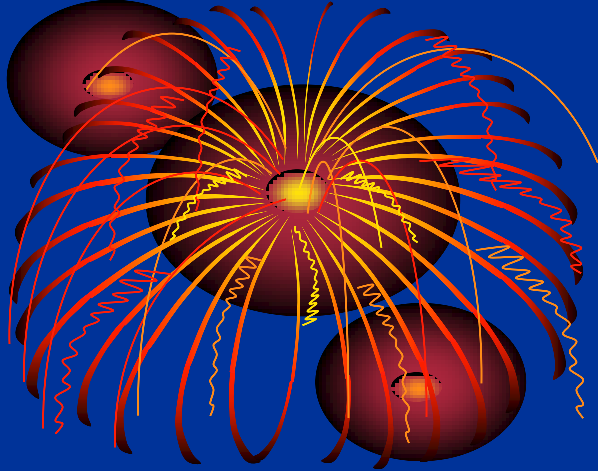

- FLT (DNA Synthesis)
- ^{60}Cu-ATSM, ^{18}F-EF5, ^{18}F-FMISO
- (Assessment for hypoxia)
- FIAU, FHBG, FHPG (Gene therapy)
- ^{11}C-Acetate (Slow growing tumors)
- ^{18}F or ^{11}C -labeled Choline
- (Slow growing tumors)
- ^{18}F-Fuoride (Bone imaging)

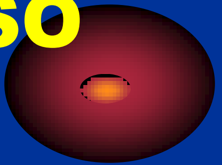

Imaging of Non-small Cell Lung Cancer

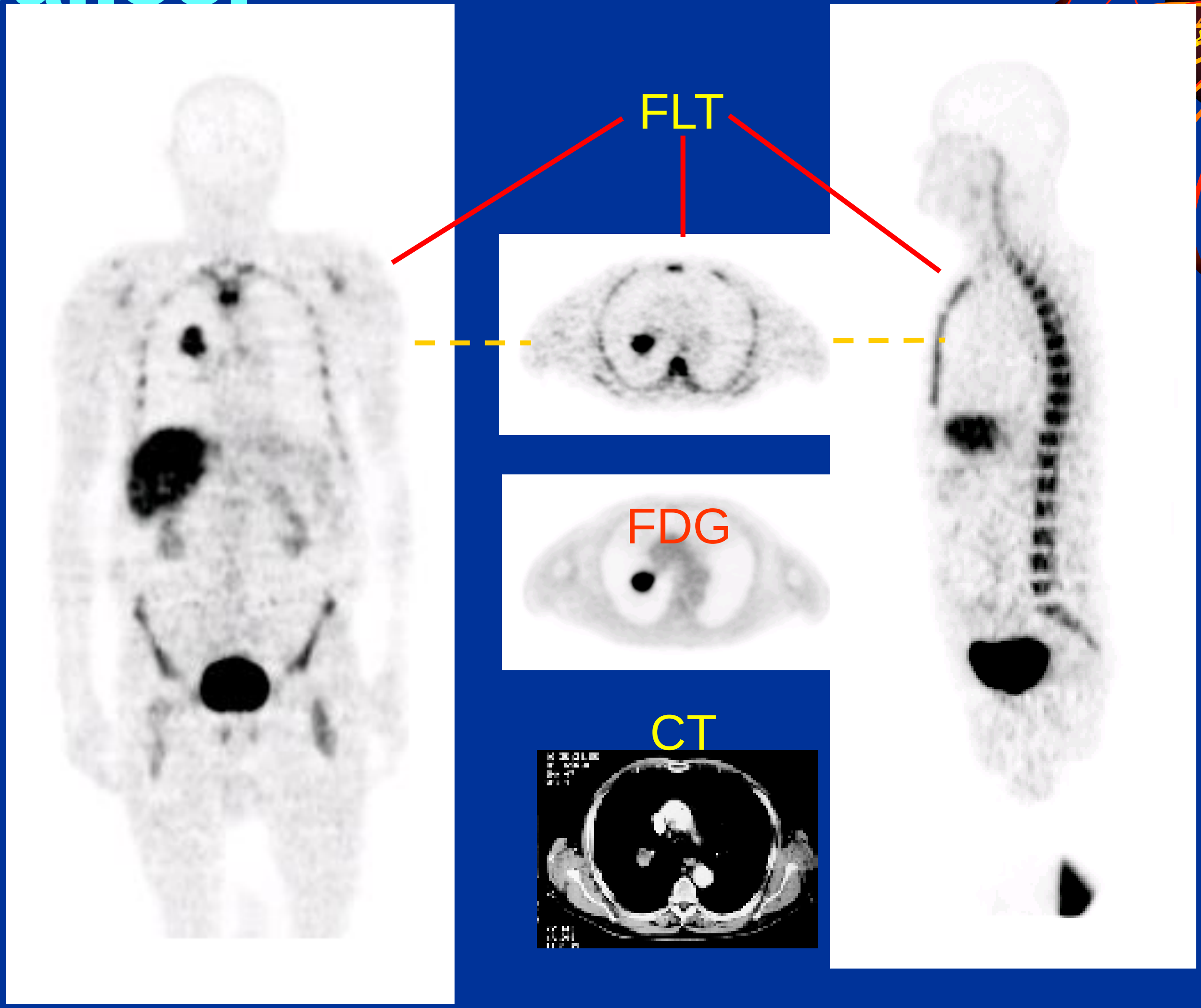

AF Shields, JR Grierson, BM Dohmen, H-J Machulla et al.
Nature Med 4:1334, 1998

90 Minutes

MRI Post-GAD Sequence

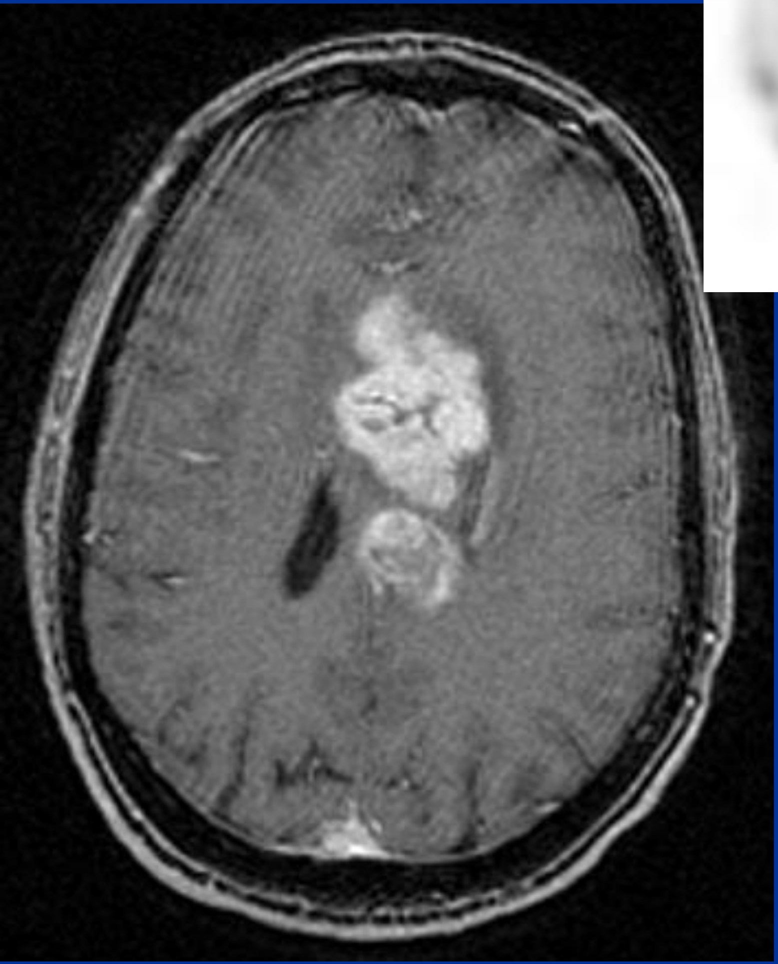

^{18}F-EF5 PET

Evans,Koch 2005

MR-PET Fusion

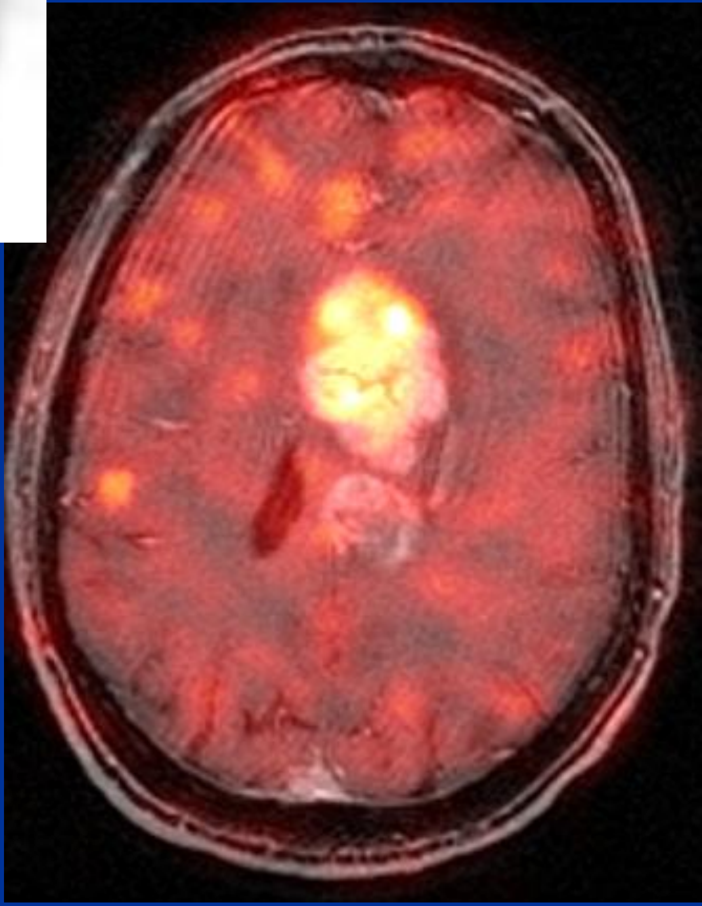

Comparison of Average SUVmean-asc

- **The mean±SD of SUVmean-arch for healthy and non-healthy subjects were 0.83±0.20 and 1.02±0.29, respectively; and this difference was significant (P value<0.001). The spearman CC of healthy and non-healthy subjects were 0.37 (P=0.001) and 0.67 (P<0.001), respectively. The trend-lines for both groups are shown below.**

SUVmean-asc(healthy)

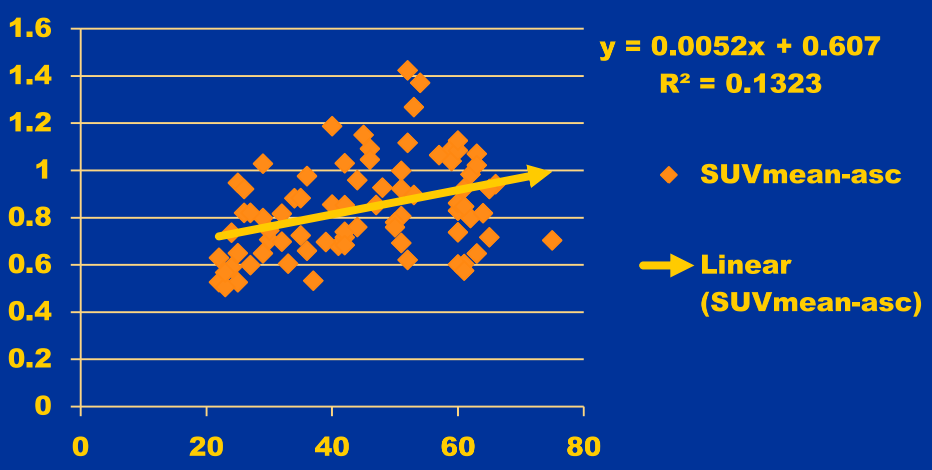

SUVmean-asc(non-healthy)

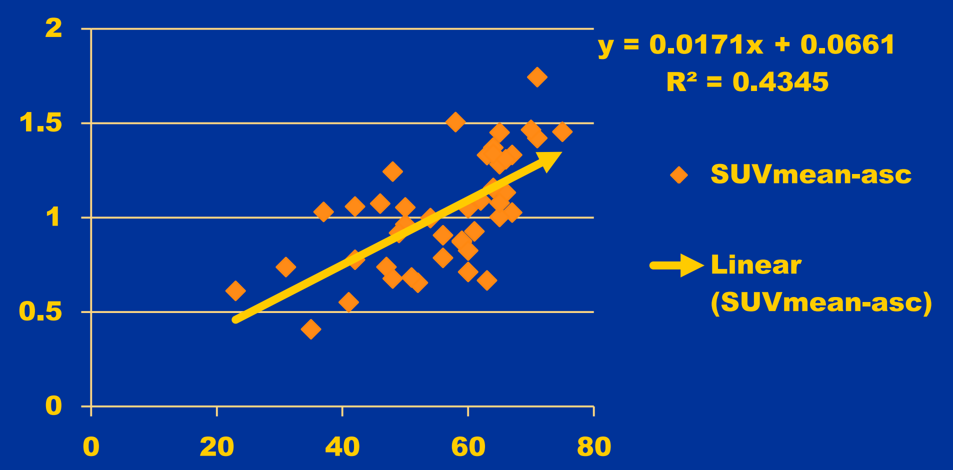

Global cardiac ^{18}F-NaF uptake

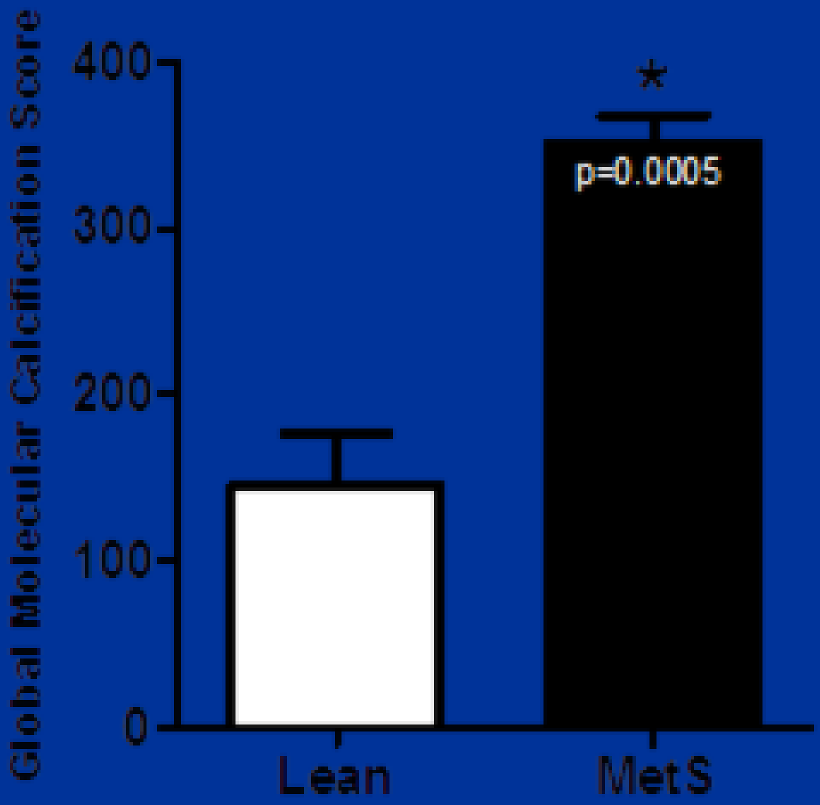

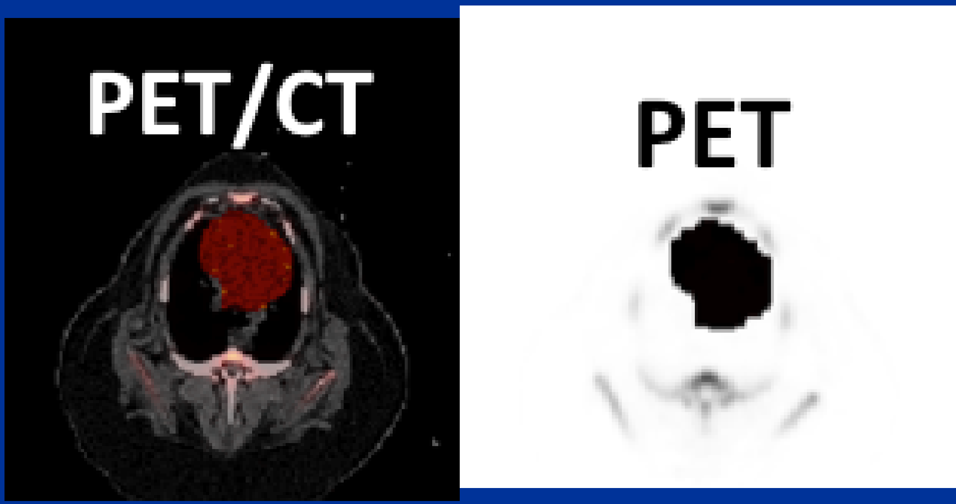

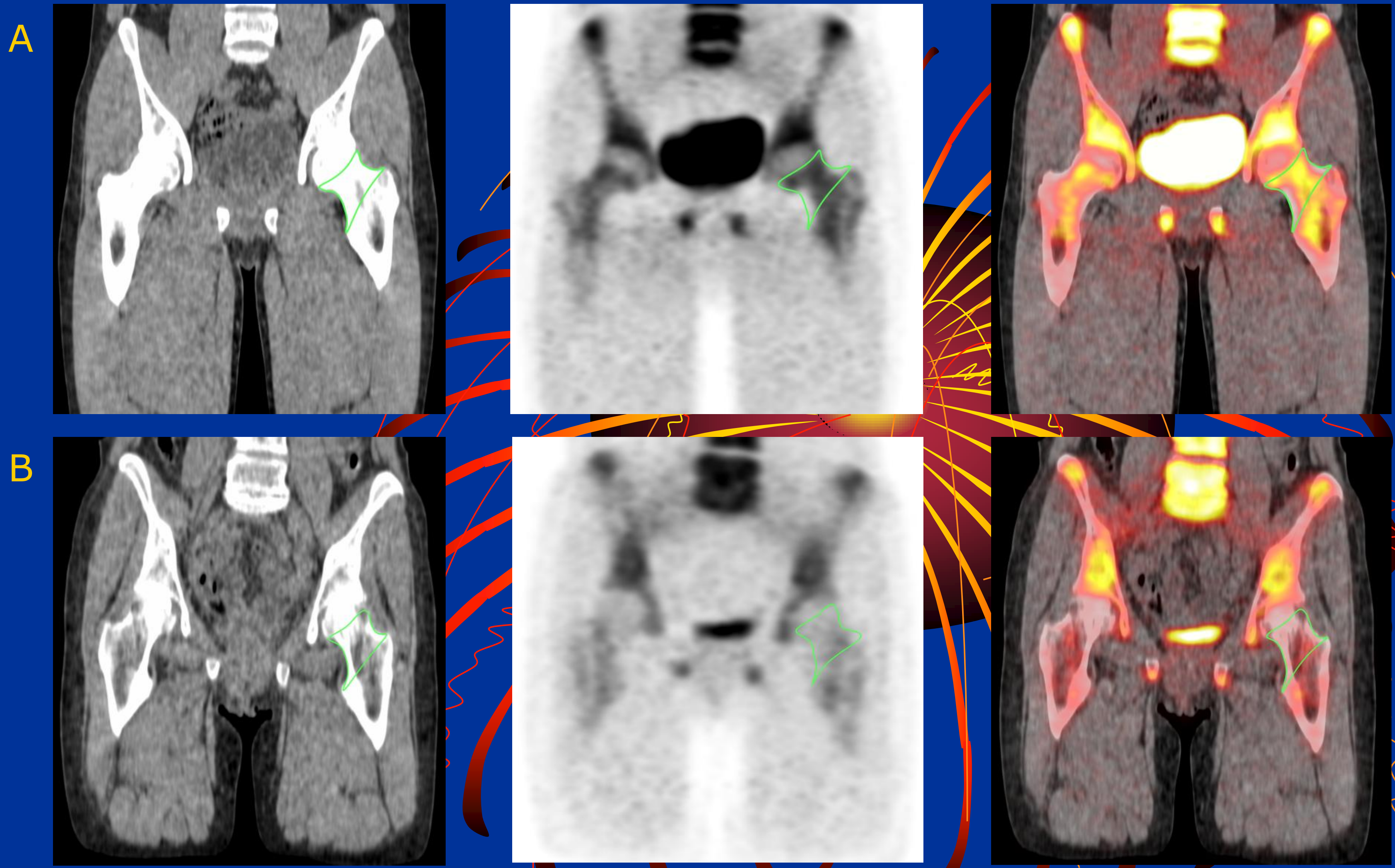

The CT, PET, and PET/CT images shown above from two normal subjects, a 28 year-old male (A) and a 64 year-old female (B). The femoral neck activity is anatomically defined with the medial boundaries based on the epiphyseal line and lateral boundaries by the intertrochanteric ridge. Based on this delineation, quantitative metrics were generated in both subjects. Total calcium metabolism (TCM = SUVmean*metabolically active volume) in patient (A) was 6715.79 while TCM in patient (B) was 2587.44.

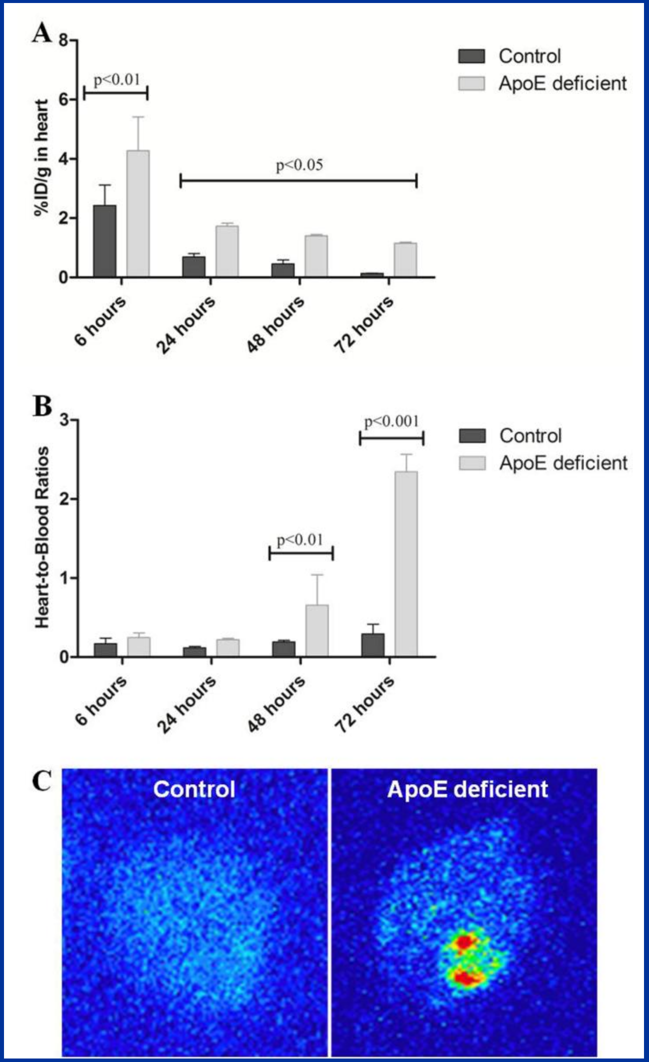

FIGURE 5. Heart uptake and DAR from control and apoE -/- mice. (A) Mean heart uptake obtained after intravenous administration of [^{125}I]IONPs into healthy and atherosclerotic mice (n=4). (B) Mean heart-to-blood ratios obtained after intravenous administration of [^{125}I]IONPs into healthy and atherosclerotic mice (n=4). (C) DAR obtained from heart of healthy and atherosclerotic mice, respectively, at 72 h post-injection of [^{125}I]IONPs (20 μCi, 0.8 mg Fe/kg).

Philips Ingenuity TF PET/MR

Sequential PET and MR imaging

CE Mark in Europe
FDA 510(k) clearance in US

http://multivu.prnewswire.com/mnr/philips/48197/

Potentional Future Applications

Neurological Disorders and Diseases

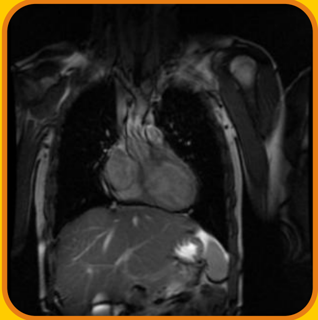

Cardiovascular Disorders and Diseases

Musculoskeletal Disorders and Diseases

Fusion Imaging of PET and MRI
Metabolic Function in In-vivo Human Brainstem

Mammillary Body
Red Nucleus
Dorsal Raphe
Thalamus
Inferior Colliculus

Fusion PET-MRI

Centralis Superior

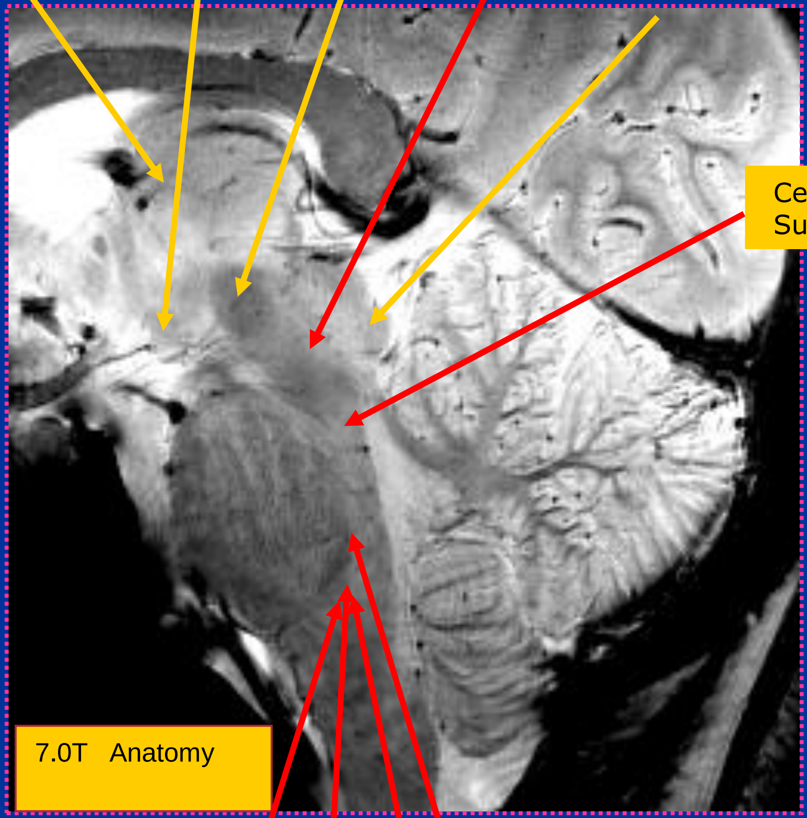

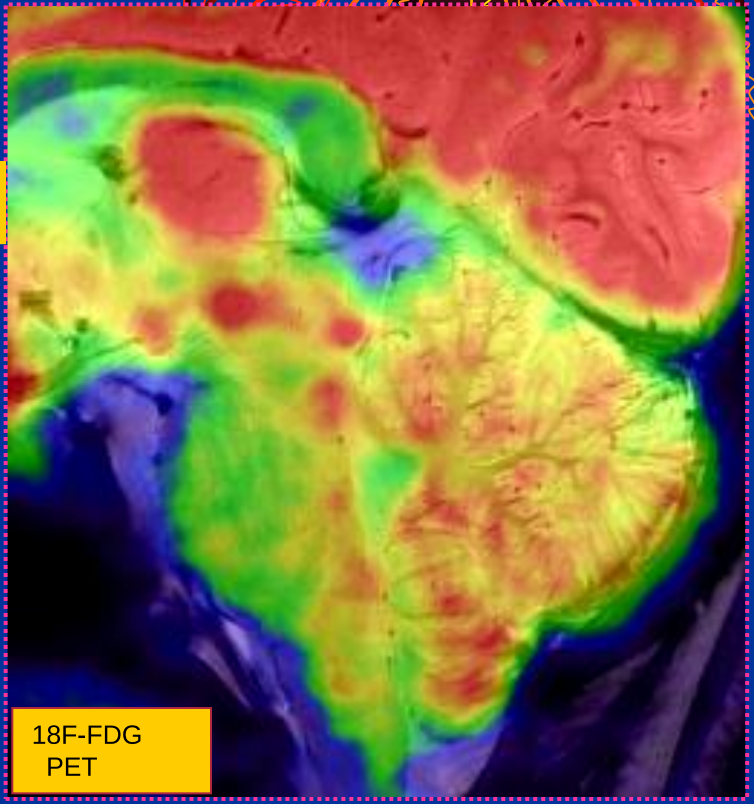

PET-MRI Fusion

Raphe Pontis
Raphe-Magnus, Obscurus, Pallidus

Anatomy Obtained by 7.0T MRI

SUVR of Glucose Metabolism
By Fusion PET-MRI

FDG PET/CT in Cardiac Sarcoidosis

Cardiac MRI

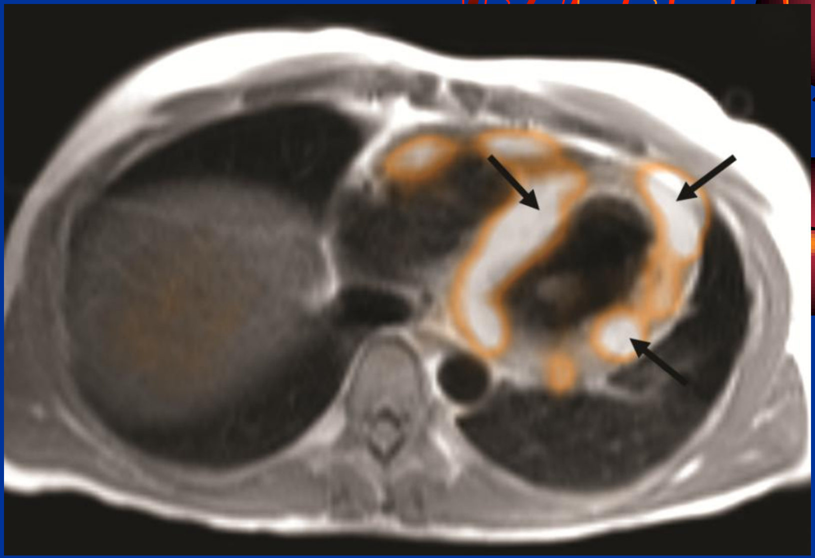

FDG PET/MRI

Images in a 51-year-old man with history of cardiac dysrhythmias and sarcoidosis who underwent evaluation for cardiac involvement.
Axial software-fused FDG PET/MR image of heart demonstrates heterogeneously increased FDG uptake (arrows) in left ventricular myocardium.

Torigian DA et al. Radiology. 2013 Apr;267(1):26-44.

FDG-PET/CT in Diabetic Foot

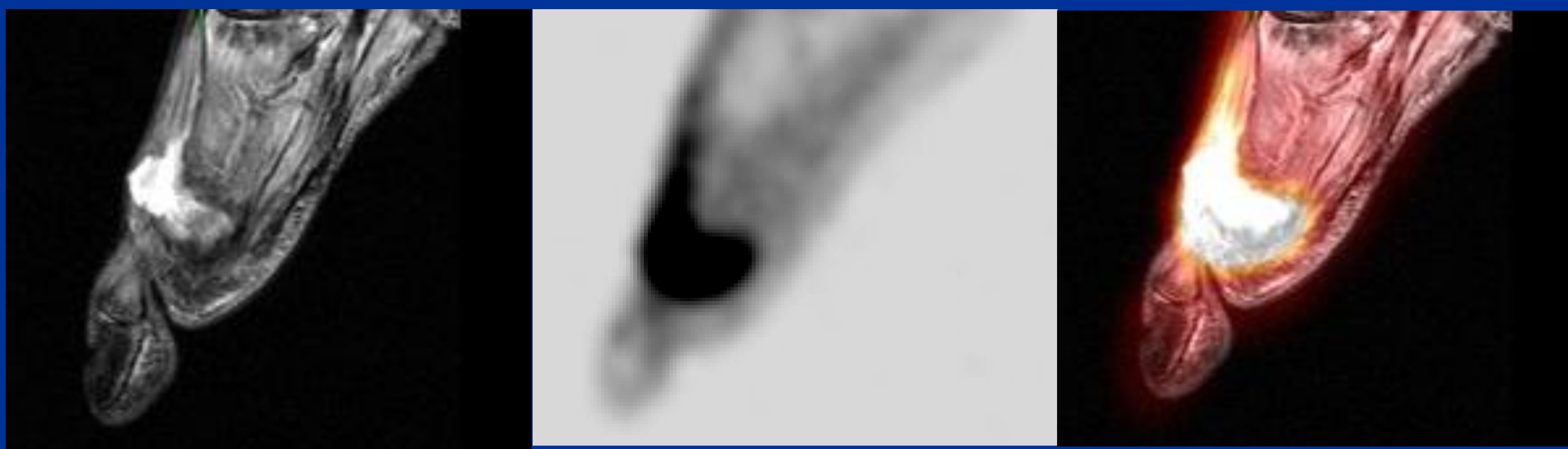

Hochhold J et al. Society of Nuclear Medicine; 2005.

Imaging Plaques and Tangles in Patients with Cognitive Impairment

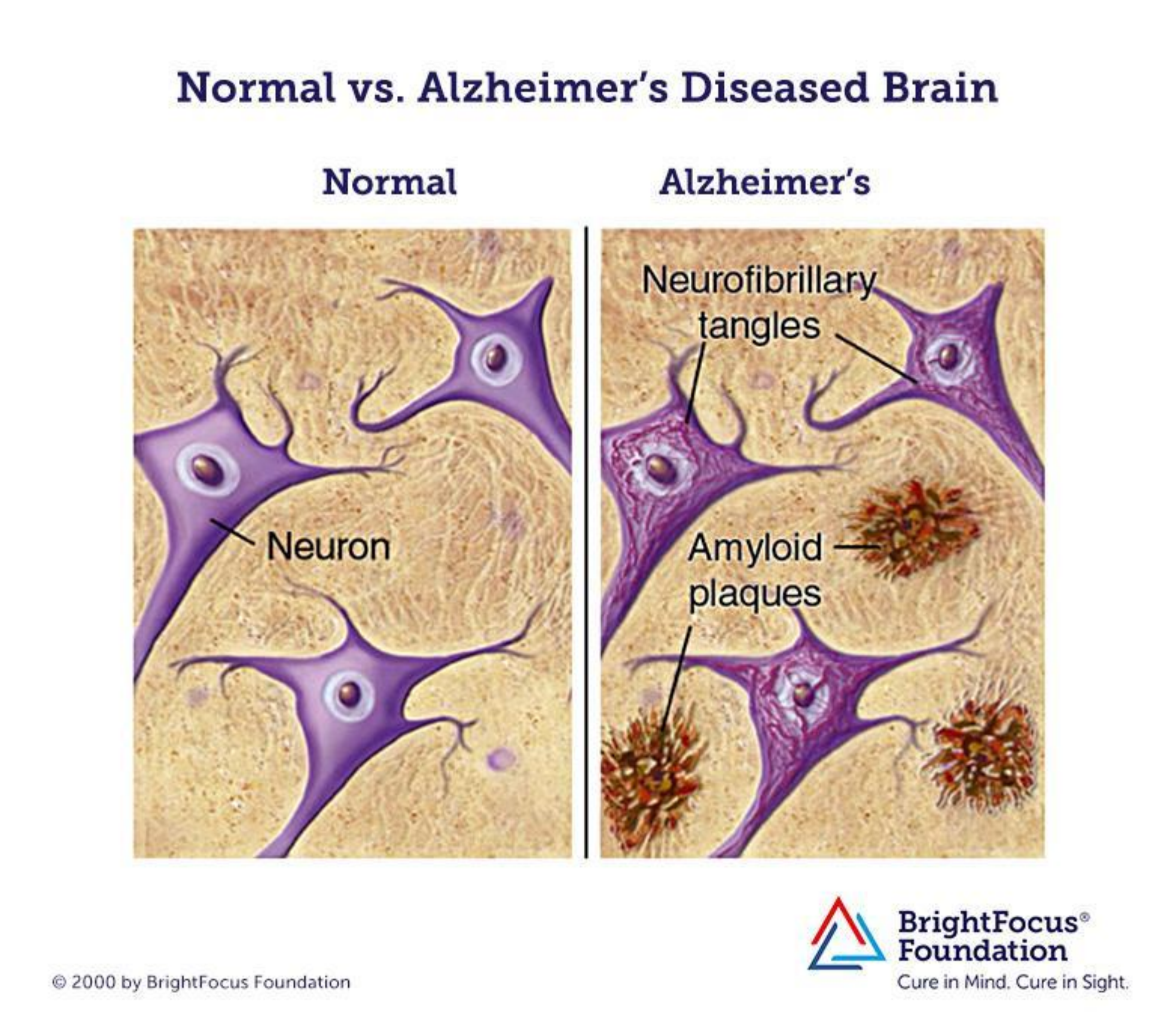

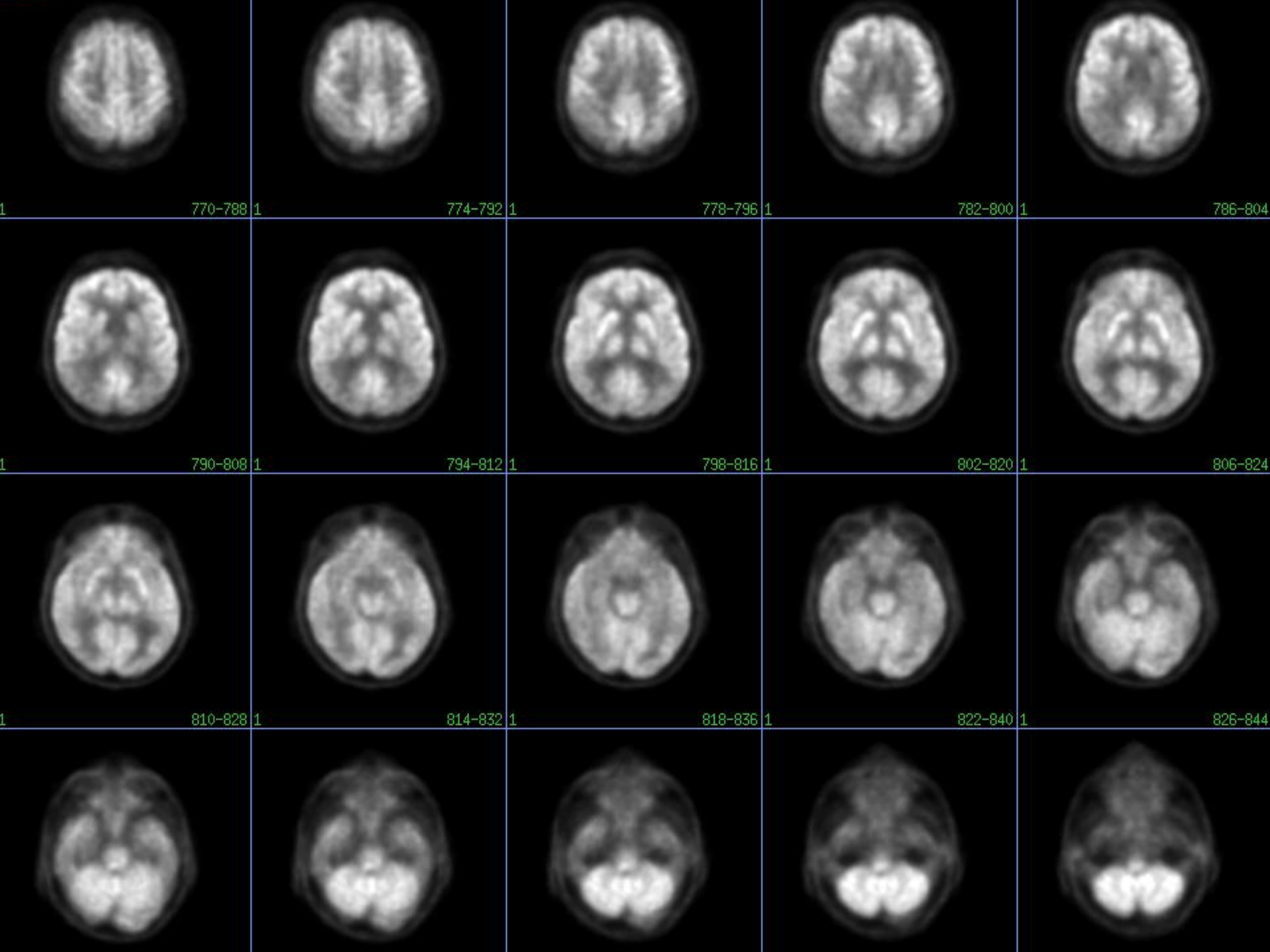
1
770-788
1
774-792
1
778-796
1
782-800
1
786-804
1
790-808
1
794-812
1
798-816
1
802-820
1
806-824
1
810-828
1
814-832
1
818-836
1
822-840
1
826-844

PiB

FDG

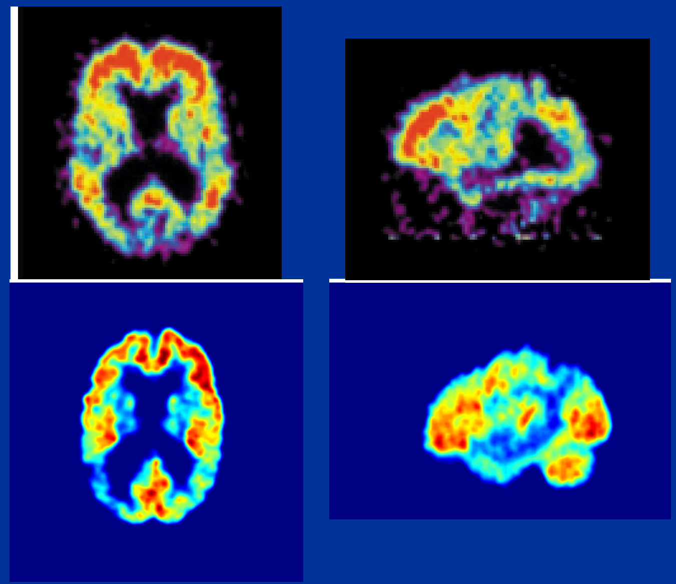

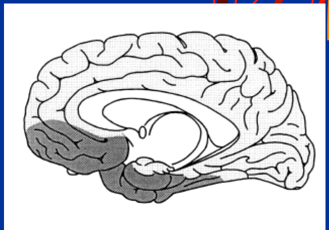

BRAAK AND BRAAK

CORTICAL DESTRUCTION IN ALZHEIMER'S DISEASE

Neurobiology of Aging, Vol. 18, No. 4, pp 351–357, 1997

0197-4580/97 $17.00 + .00

Imaging (PET)

Pathology

- FDG-PET-CT Imaging has had a substantial impact on research and on the day to day practice of medicine. This has resulted in minimizing pain and suffering for millions of patients with serious diseases/disorders and in reducing cost of health care worldwide.

Thank You

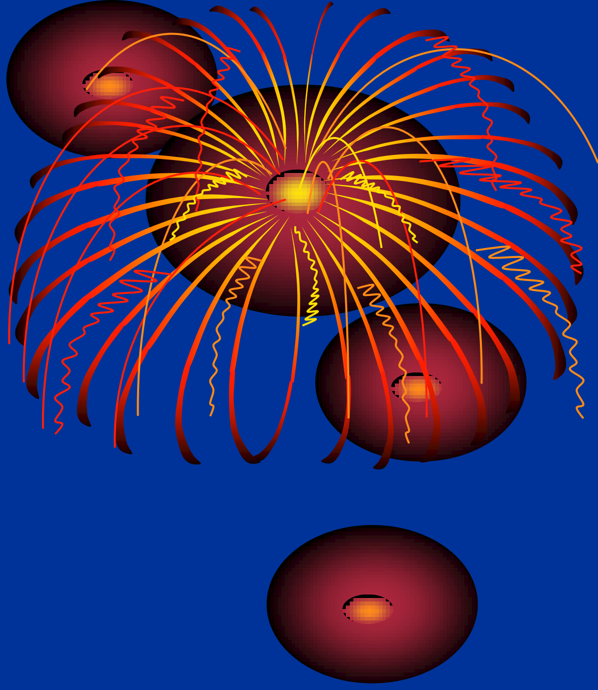

Thank you